# Supplementary material

## Supplementary Figure 1

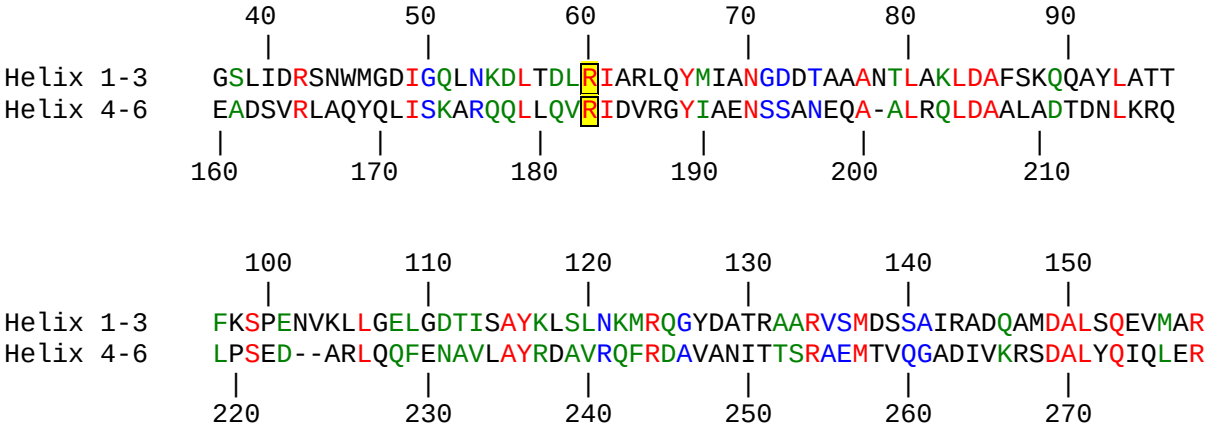


**Legend to Supplementary Figure 1) Alignment of the McpS-LBR sequence fragment which forms helices α1-α3 (amino acids 37-158 of McpS) with the fragment that forms helices α4-α6 (amino acids 160-278).** The sequence alignment was done using the CLUSTALW algorithm (Thompson *et al.*, 1997, Nucleic Acids Res. 24, 4876) of the NPSA server (http://npsa-pbil.ibcp.fr/cgi-bin/npsa_automat.pl?page=/NPSA/npsa_clustalw.html) using a gap opening penalty of 10 and a gap extension penalty of 0.1. Arg60 and Arg183 which form direct interactions with malate and acetate, respectively, are shaded in yellow.

## Supplementary Figure 2

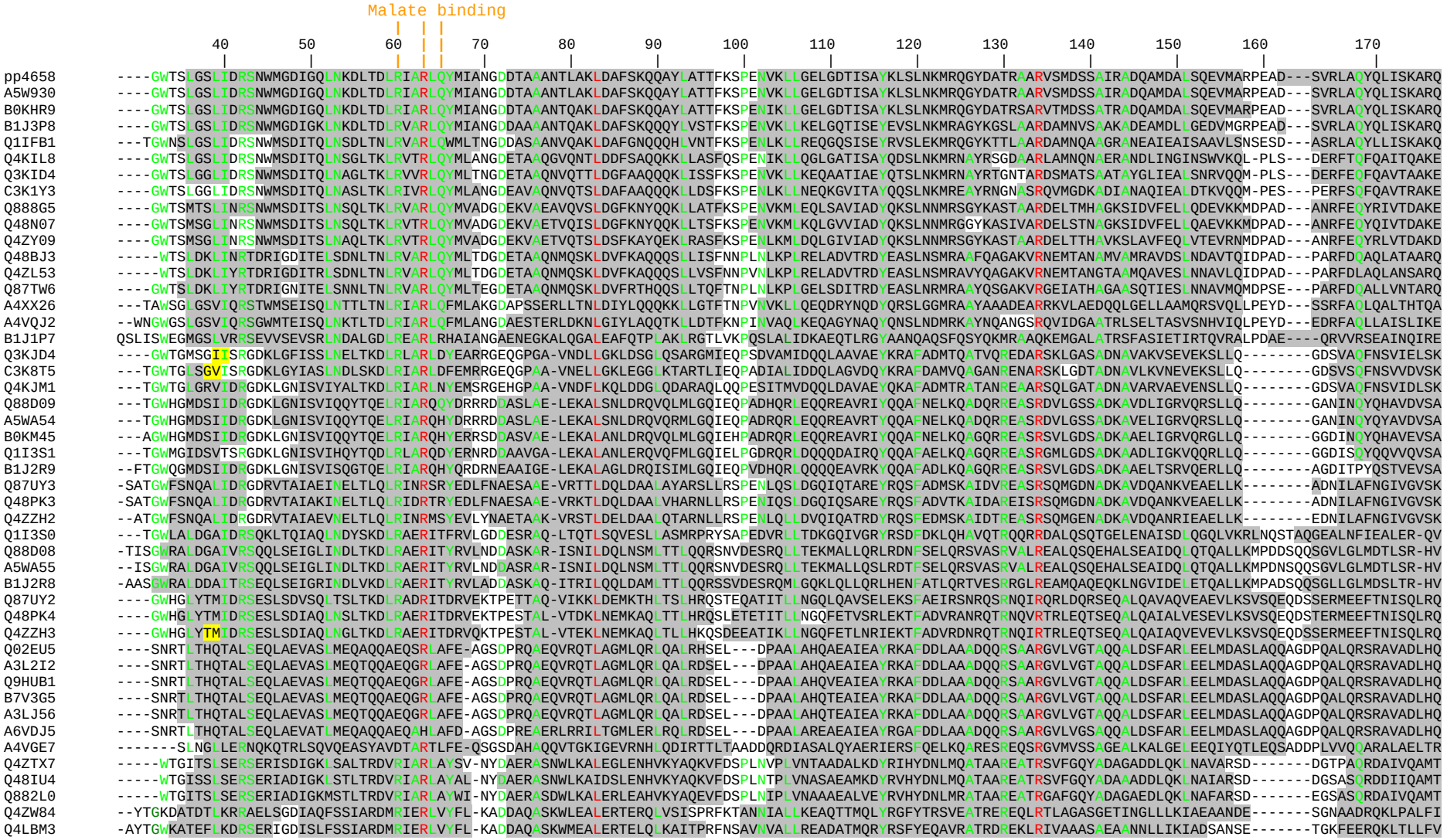

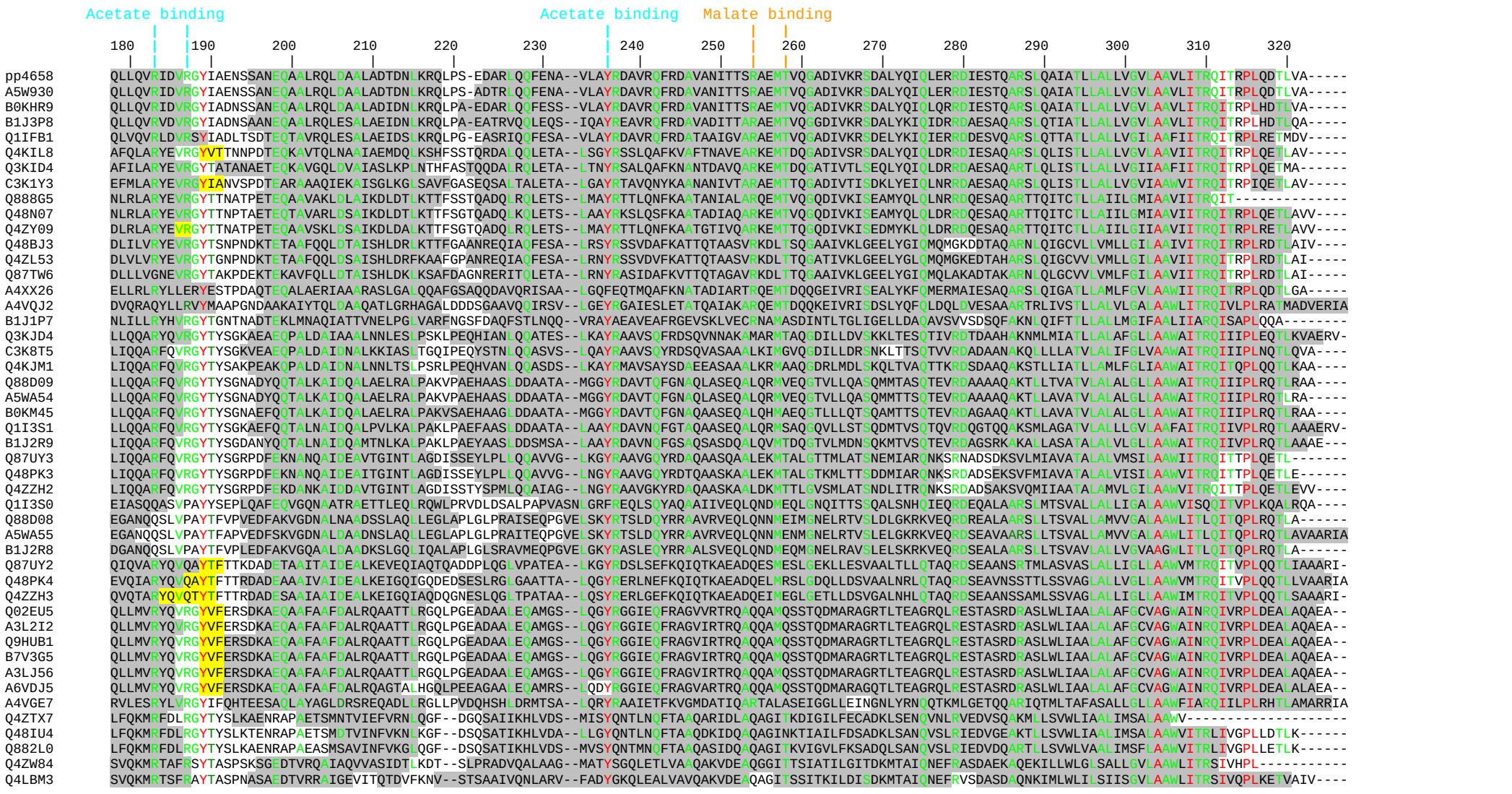
Acetate binding
Acetate binding
Malate binding
180
190
200
210
220
230
240
250
260
270
280
290
300
310
320
pp4658 QLLQVRIDVRGYIAENSSANEQAALRQLDAALADTDNLKRQLPS-EDARLQQFENA--VLAYRDAVRQFRDAVANITTSRAEMTVQGADIVKRSDALYQIQLERRDIESTQARSLQAIATLLALLVGVLAAVLITRQITRPLQDTLVA-----
A5W930 QLLQVRIDVRGYIAENSSANEQAALRQLDAALADTDNLKRQLPS-ADTRLQQFENA--VLAYRDAVRQFRDAVANITTSRAEMTVQGADIVKRSDALYQIQLERRDIESTQARSLQAIATLLALLVGVLAAVLITRQITRPLQDTLVA-----
B0KHR9 QLLQVRIDVRGYIADNSSANEQAALRQLDAALADIDNLKRQLPA-EDARLQQFESS--VLAYRDAVRQFRDAVANITTSRAEMTVQGADIVKRSDALYQIQLQRRDIESTQARSLQAIATLLALLVGVLAAVLITRQITRPLHDTLVA-----
B1J3P8 QLLQVRVDVRGYIADNSAANEQAALRQLESALAEIDNLKRQLPA-EATRVQQLEQS--IQAYREAVRQFRDAVADITTARAEMTVQGGDIVKRSDALYKIQIDRRDAESAQARSLQTIATLLALLVGVLAAVLITRQITRPLHDTLQA-----
Q1IFB1 QLVQVRLDVRSYIADLTSDTEQTAVRQLESALAEIDSLKRQLPG-EASRIQQFESA--VLAYRDAVRQFRDATAAIGVARAEMTVQGADIVKRSDELYKIQIERRDDESVQARSLQTTATLLALLVGILAAFIITRQITRPLRETMDV-----
Q4KIL8 AFQLARYEVRGYVTTNNPDTEQKAVTQLNAAIAEMDQLKSHFSSTQRDALQQLETA--LSGYRSSLQAFKVAFTNAVEARKEMTDQGADIVSRSDALYQIQLDRRDIESAQARSLQLISTLALLVGVLAAVIITRQITRPLQETLAV-----
Q3KID4 AFILARYEVRGYTATANAETEQKAVGQLDVAIASLKPLNTHFASTQQDALRQLETA--LTNYRSALQAFKNANTDAVQARKEMTDQGATIVTLSEQLYQIQLDRRDAESAQARTLQLISTLALLVGIIAAFIITRQITRPLQETMA------
C3K1Y3 EFMLARYEVRGYIANVSPDTEARAAAQIEKAISGLKGLSAVFGASEQSALTALETA--LGAYRTAVQNYKAANANIVTARAEMTTQGADIVTISDKLYEIQLNRRDAESAQARSLQLISTLALLVGVIAAWVITRQITRPIQETLAV-----
Q888G5 NLRLARYEVRGYTTNATPETEQAAVAKLDLAIKDLDTLKTTFSSTQADQLRQLETS--LMAYRTTLQNFKAATANIALARQEMTVQGQDIVKISEAMYQLQLNRRDQESAQARTTQITCTLLAIILGMIAAVIITRQIT--------------
Q48N07 NLRLARYEVRGYTTNPTAETEQTAVARLDSAIKDLDTLKTTFSGTQADQLKQLETS--LAAYRKSLQSFKAATADIAQARKEMTVQGQDIVKISEAMYQLQLRDRDQESAQARTTQITCTLLAIILGMIAAVIITRQITRPLQETLAVV----
Q4ZY09 DLRLARYEVRGYTTNATPETEQAAVSKLDSAIKDLDALKTTFSGTQADQLRQLETS--LMAYRTTLQNFKAATGTIVQARKEMTTQGQDIVKISEDMYKLQLDRRDQESAQARTTQITCTLLAIILGIIAAVIITRQITRPLRETLAVV----
Q48BJ3 DLILVRYEVRGYTSNPNDKTETAAFQQLDTAISHLDRLKTTFGAANREQIAQFESA--LRSYRSSVDAFKATTQTAASVRKDLTSQGAAIVKLGEELYGIQMQMGKDDTAQARNLQIGCVLLVMLLGILAAIVITRQITRPLRDTLAIV----
Q4ZL53 DLVLVRYEVRGYTGNPNDKTETAAFQQLDSAISHLDRFKAAFGPANREQIAQFESA--LRNYRSSVDVFKATTQTAASVRKDLTTQGATIVKLGEELYGLQMQMGKEDTAHARSLQIGCVVLVMLLGILAAVIITRQITRPLRDTLAI-----
Q87TW6 DLLLVGNEVRGYTAKPDEKTEKAVFQLDTAISHLDKLKSAFDAGNRERITQLETA--LRNYRASIDAFKVTTQTAGAVRKDLTTQGAAIVKLGEELYGIQMQLAKADTAKARNLQLGCVVLVMLFGILAAVIITRQITRPLRDTLAI-----
A4XX26 ELLRLRYLLERYESTPDAQTEQALAERIAAARASLGALQQAFGSAQQDAVQRISAA--LGQFEQTMQAFKNATADIARTRQEMTDQQGEIVRISEALYKFQMERMAIESAQARSLQIGATLLAMLFGVLAAWIITRQITRPLQDTLGA-----
A4VQJ2 DVQRAQYLLRVYMAAPGNDAAKAIYTQLDAAQATLGRHAGALDDDSGAAVQQIRSV--LGEYRGAIESLETATQAIAKARQEMTDQQKEIVRISDSLYQFQLDQLDVESAAARTRLIVSTLLALVLGALAAWLITRQIVLPLRATMADVERIA
B1J1P7 NLILLRYHVRGYTGNTNADTEKLMNAQIATTVNELPGLVARFNGSFDAQFSTLNQQ--VRAYAEAVEAFRGEVSKLVECRNAMASDINTLTGLIGELLDAQAVSVVSDSQFAKNLQIFTTLLALLMGIFAALIIARQISAPLQQA--------
Q3KJD4 LLQQARYQVRGYTYSGKAEAEQPALDAIAAALNNLESLPSKLPEQHIANLQQATES--LKAYRAAVSQFRDSQVNNAKAMARMTAQGDILLDVSKKLTESQTIVRDTDAAHAKNMLMIATLLALAFGLLAAWAITRQIIIPLEQTLKVAERV-
C3K8T5 LIQQARFQVRGYTYSGKVEAEQPALDAIDNALKKIASLTGQIPEQYSTNLQQASVS--LQAYRAAVSQYRDSQVASAAALKIMGVQGDILLDRSNKLTTSQTVVRDADAANAKQLLLLATVLALIFGLVAAWAITRQIIIPLNQTLQVA----
Q4KJM1 LIQQARFQVRGYTYSAKPEAKQPALDAIDNALNNLTSLPSRLPEQHVANLQQASDS--LKAYRMAVSAYSDAEEASAAALKRMAAQGDRLMDLSKQLTVAQTTKRDSDAAQAKSTLLIATLLAMLFGLIAAWAITRQITQPLQQTLKAA----
Q88D09 LLQQARFQVRGYTYSGNADYQQTALKAIDQALAELRALPAKVPAEHAASLDDAATA--MGGYRDAVTQFGNAQLASEQALQRMVEQGTVLLQASQMMTASQTEVRDAAAAQAKTLLTVATVLALALGLLAAWAITRQIIIPLRQTLRAA----
A5WA54 LLQQARFQVRGYTYSGNADYQQTALKAIDQALAELRALPAKVPAEHAASLDDAATA--MGGYRDAVTQFGNAQLASEQALQRMVEQGTVLLQASQMMTTSQTEVRDAAAAQAKTLLAVATVLALALGLLAAWAITRQIIIPLRQTLRA-----
B0KM45 LLQQARFQVRGYTYSGNAEFQQTALKAIDQALAELRALPAKVSAEHAAGLDDAATA--MGGYRDAVTQFGNAQAASEQALQHMAEQGTLLLQTSQAMTTSQTEVRDAGAAQAKTLLAVATVLALALGLLAAWAITRQIIIPLRQTLRAA----
Q1I3S1 LLQQARFQVRGYTYSGKAEFQQTALNAIDQALPVLKALPAKLPAEFAASLDDAATA--LAAYRDAVNQFGTAQAASEQALQRMSAQGQVLLSTSQDMTVSQTQVRDQGTQQAKSMLAGATVLALLLGVLAAFAITRQIIVPLRQTLAAAERV-
B1J2R9 LIQQARFQVRGYTYSGDANYQQTALNAIDQAMTNLKALPAKLPAEYAASLDDSMSA--LAAYRDAVNQFGSAQSASDQALQVMTDQGTVLMDNSQKMTVSQTEVRDAGSRKAKALLASATALALVLGLLAAWAITRQIIVPLRQTLAAAE---
Q87UY3 LIQQARFQVRGYTYSGRPDFEKNANQAIDEAVTGINTLAGDISSEYLPLLQQAVVG--LKGYRAAVGQYRDAQAASQAALEKMTALGTTMLATSNEMIARQNKSRNADSDKSVLMIAVATALALVMSILAAWIITRQITTPLQETL-------
Q48PK3 LIQQARFQVRGYTYSGRPDFEKNANQAIDEAITGINTLAGDISSEYLPLLQQAVVG--LNGYRAAVGQYRDTQAASKAALEKMTALGTKMLTTSDDMIARQNKSRDADSEKSVFMIAVATALALVISILAAWVITRQITTPLQETLE------
Q4ZZH2 LIQQARFQVRGYTYSGRPDFEKDANKAIDDAVTGINTLAGDISSTYSPMLQQAIAG--LNGYRAAVGKYRDAQAASKAALDKMTTLGVSMLATSNDLITRQNKSRDADSAKSVQMIIAATALAMVLGILAAWVITRQITTPLQETLEVV----
Q1I3S0 EIASQQASVPAYYSEPLQAFEQVGQNAATRAETTLEQLRQWLPRVDLDSALPAPVASNLGRFREQLSQYAQAAIIVEQLQNDMEQLGNQITTSSQALSNHQIEQRDEQALAARSLMTSVALLALLIGALAAWVISQQITVPLKQALRQA----
Q88D08 EGANQQSLVPAYTFVPVEDFAKVGDNALNAADSSLAQLLEGLAPLGLPRAISEQPGVELSKYRTSLDQYRRAAVRVEQLQNNMEIMGNELRTVSLDLGKRKVEQRDREALAARSLLTSVALLAMVVGALAAWLITLQITQPLRQTLA------
A5WA55 EGANQQSLVPAYTFAPVEDFSKVGDNALDAADNSLAQLLEGLAPLGLPRAITEQPGVELSKYRTSLDQYRRAAVRVEQLQNNMENMGNELRTVSLELGKRKVEQRDSEAVAARSLLTSVALLAMVVGALAAWLITLQITQPLRQTLAVAARIA
B1J2R8 DGANQQSLVPAYTFVPLEDFAKVGQAALDAADKSLGQLIQALAPLGLSRAVMEQPGVELGKYRASLEQYRRAALSVEQLQNDMEQMGNELRAVSLELSKRKVEQRDSEALAARSLLTSVAVLALLVGVAAGWLITLQITQPLRQTLA------
Q87UY2 QIQVARYQVQAYTFTTKDADETAAITAIDEALKEVEQIAQTQADDPLQGLVPATEA--LKGYRDSLSEFKQIQTKAEADQESMESLGEKLLESVAALTLLQTAQRDSEAANSRTMLASVASLALLIGLLAAWVMTRQITVPLQQTLIAAARI-
Q48PK4 EVQIARYQVQAYTFTTRDADEAAAIVAIDEALKEIGQIGQDEDSESLRGLGAATTA--LQGYRERLNEFKQIQTKAEADQELMRSLGDQLLDSVAALNRLQTAQRDSEAVNSSTTLSSVAGLALLVGLLAAWVMTRQITVPLQQTLLVAARIA
Q4ZZH3 QVQTARYQVQTYTFTTRDADESAAIAAIDEALKEIGQIAQDQGNESLQGLTPATAA--LQSYRERLGEFKQIQTKAEADQEIMEGLGETLLDSVGALNHLQTAQRDSEAANSSAMLSSVAGLALLIGLLAAWIMTRQITVPLQQTLSAAARI-
Q02EU5 QLLMVRYQVRGYVFERSDKAEQAAFAAFDALRQAATTLRGQLPGEADAALEQAMGS--LQGYRGGIEQFRAGVVRTRQAQQAMQSSTQDMARAGRTLTEAGRQLRESTASRDRASLWLIAALALAFGCVAGWAINRQIVRPLDEALAQAEA--
A3L2I2 QLLMVRYQVRGYVFERSDKAEQAAFAAFDALRQAATTLRGQLPGEADAALEQAMGS--LQGYRGGIEQFRAGVIRTRQAQQAMQSSTQDMARAGRTLTEAGRQLRESTASRDRASLWLIAALALAFGCVAGWAINRQIVRPLDEALAQAEA--
Q9HUB1 QLLMVRYQVRGYVFERSDKAEQAAFAAFDALRQAATTLRGQLPGEADAALEQAMGS--LQGYRGGIEQFRAGVIRTRQAQQAMQSSTQDMARAGRTLTEAGRQLRESTASRDRASLWLIAALALAFGCVAGWAINRQIVRPLDEALAQAEA--
B7V3G5 QLLMVRYQVRGYVFERSDKAEQAAFAAFDALRQAATTLRGQLPGEADAALEQAMGS--LQGYRGGIEQFRAGVIRTRQAQQAMQSSTQDMARAGRTLTEAGRQLRESTASRDRASLWLIAALALAFGCVAGWAINRQIVRPLDEALAQAEA--
A3LJ56 QLLMVRYQVRGYVFERSDKAEQAAFAAFDALRQAATTLRGQLPGEADAALEQAMGS--LQGYRGGIEQFRAGVIRTRQAQQAMQSSTQDMARAGRTLTEAGRQLRESTASRDRASLWLIAALALAFGCVAGWAINRQIVRPLDEALAQAEA--
A6VDJ5 QLLMVRYQVRGYVFERSDKAEQAAFAAFDALRQAGTALHGQLPEEAGAALEQAMRS--LQDYRGGIEQFRAGVARTRQAQQAMQSSTQDMARAGQTLTEAGRQLRESTASRDRASLWLIAALALAFGCVAGWAINRQIVRPLDEALALAEA--
A4VGE7 RVLESRYLVRGYIFQHTEESAQLAYAGLDRSREQADLLRGLLPVDQHSHLDRMTSA--LQRYRAAIETFKVGMDATIQARTALASEIGGLLEINGNLYRNQQTKMLGETQQARIQTMLTAFASALLGLLAAWFIARQIILPLRHTLAMARRIA
Q4ZTX7 LFQKMRFDLRGYTYSLKAENRAPAETSMNTVIEFVRNLQGF--DGQSAIIKHLVDS--MISYQNTLNQFTAAQARIDLAQAGITKDIGILFECADKLSENQVNLRVEDVSQAKMLLSVWLIAALIMSALAAWV----------
Q48IU4 LFQKMRFDLRGYTYSLKTENRAPAETSMDTVINFVKNLKGF--DSQSATIKHLVDA--LLGYQNTLNQFTAAQDKIDQAQAGINKTIAILFDSADKLSANQVSLRIEDVGEAKTLLSVWLIAALIMSALAAWVITRLIVGPLLDTLK------
Q882L0 LFQKMRFDLRGYTYSLKAENRAPAEASMSAVINFVKGLQGF--DSQSATIKHLVDS--MVSYQNTMNQFTAAQASIDQAQAGITKVIGVLFKSADQLSANQVSLRIEDVDQARTLLSVWLVAALIMSFLAAWVITRLIVGPLLETLK------
Q4ZW84 SVQKMRTAFRSYTASPSKSGEDTVRQAIAQVVASIDTLKDT--SLPRADVQALAAG--MATYSGQLETLVAAQAKVDEAQGGITTSIATILGITDKMTAIQNEFRASDAEKAQEKILLWLGLSALLGVLAAWLITRSIVHPL----------
Q4LBM3 SVQKMRTSFRAYTASPNASAEDTVRRAIGEVITQTDVFKNV--STSAAIVQNLARV--FADYGKQLEALVAVQAKVDEAQAGITSSITKILDISDKMTAIQNEFRVSDASDAQNKIMLWLILSIISGVLAAWLITRSIVQPLKETVAIV----

**Legend to Supplementary Figure 2) Sequence alignment of members of the McpS-LBR like family**. The sequence of McpS-LBR (pp4658) was submitted to a BLAST search using the SwissProt/TrEMBL database. The embnet server (http://www.ch.embnet.org/software/bBLAST.html) and the blosum62 matrix were used for this search. Shown is a sequence alignment of the 47 sequences with highest sequence similarity. The sequence alignment was done using the CLUSTALW algorithm (Thompson *et al*., 1997, Nucleic Acids Res. 24, 4876) of the NPSA server (http://npsa-pbil.ibcp.fr/cgi-bin/npsa_automat.pl?page=/NPSA/npsa_clustalw.html) using a gap opening penalty of 10 and a gap extension penalty of 0.1. The degree of sequence identity/similarity is shown in red (highly conserved residues) and green (moderately conserved residues). The secondary structure for each sequence was predicted using the consensus method of the NPSA server (http://npsa-pbil.ibcp.fr/cgi-bin/npsa_automat.pl?page=/NPSA/npsa_seccons.html) using the MLRC (Guermeur *et al*., 1999, Bioinformatics 15, 413-421), DSC (King & Sternberg, 1996, Protein Sci. 5:2298-310) and PhD algorithms (Rost & Sander, 1993, J. Mol. Biol. 232, 584-99). Amino acids present in α-helical sections are shaded in grey, those predicted to form β-strand are shaded in yellow and coil/turn regions are left without shading. The amino acids which interact with malate and acetate are highlighted by orange and cyan bars, respectively, in the upper part of the alignment.

**Supplementary Figure 3)**

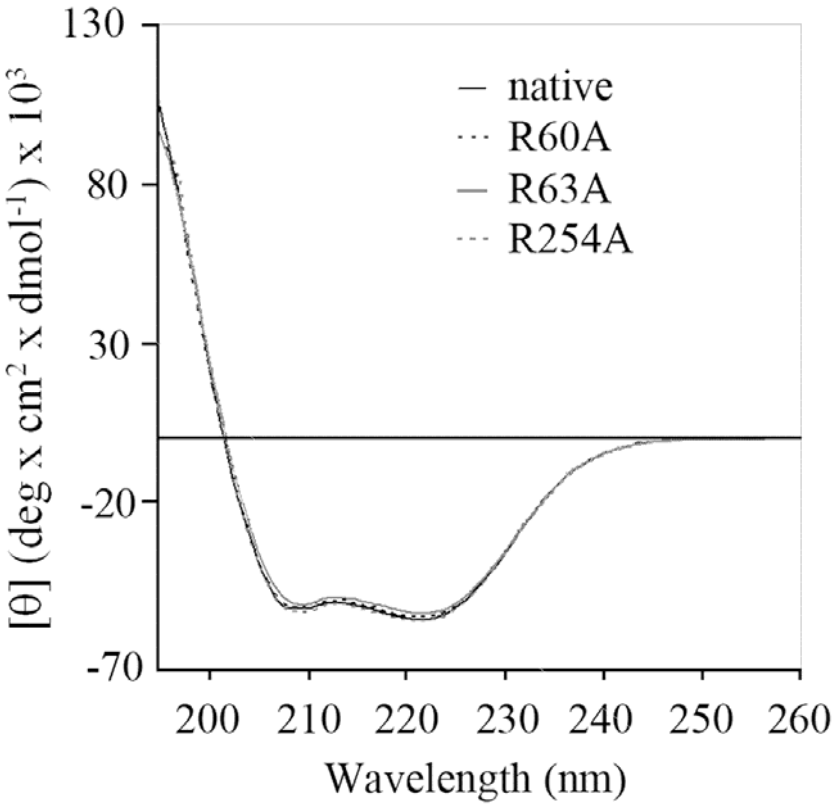


**Legend to Supplementary Figure 3) Analysis of native and mutant McpS-LBR by far uv circular dichroism spectroscopy**. Protein (0.20 mg/ml) was dialyzed against 5 mM Tris-HCl, 5 mM HEPES, 5 mM MES, pH 6.0 and spectra were recorded on a Jasco 715 spectropolarimeter (Great Dunmos, UK). Far UV spectra were recorded in quartz cells with a path length of 1 mm. Five consecutive spectra were recorded and the resulting average spectra corrected with the buffer spectrum.

**Supplementary Figure 4**

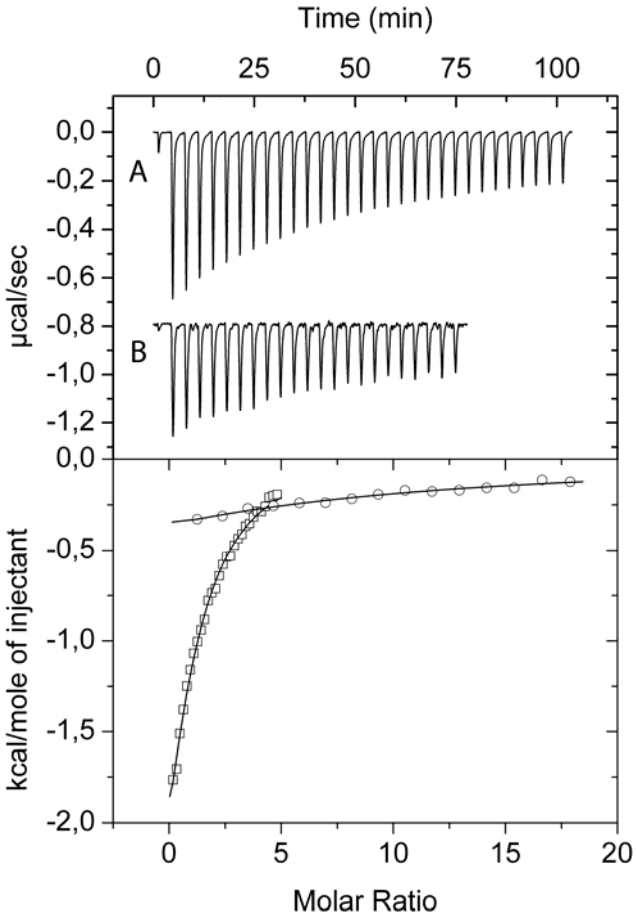


**Legend to Supplementary Figure 4) Microcalorimetric titrations of native and mutant McpS-LBR with citrate.** Upper panel: (A) Raw data for the titration of 45 µM McpS-LBR with 9.6 µl aliquots of 1 mM citrate and (B) titration of 25 µM McpS-LBR R254A with 12.8 µl aliquots of 3 mM citrate. Lower panel: Integrated, concentration-normalized and dilution heat corrected raw data. Data were fitted using the "One binding site model" of the MicroCal version of ORIGIN. □, citrate binding to native McpS-LBR, O, citrate binding to the R254A mutant. The thermodynamic parameters derived are shown in Supplementary Table 2.

**Supplementary Figure 5**

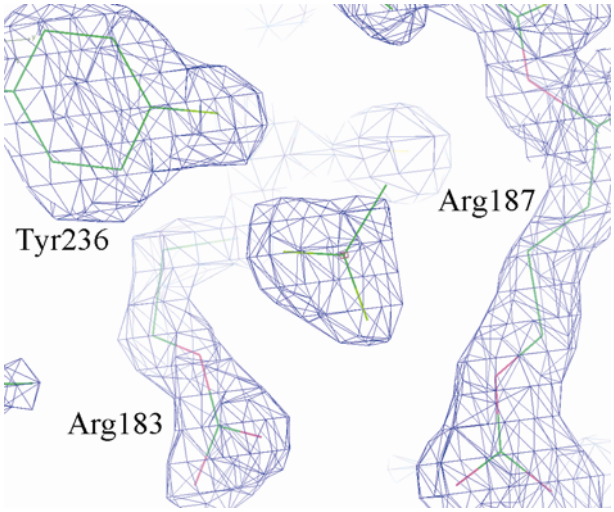


**Legend to Supplementary Figure 5) Electron density for acetate in the refined malate structure**. The McpS-LBD Sigma weighted 2Fo-Fc electron density map at a 1.8 level covering the acetate binding region.

**Supplementary Figure 6)**

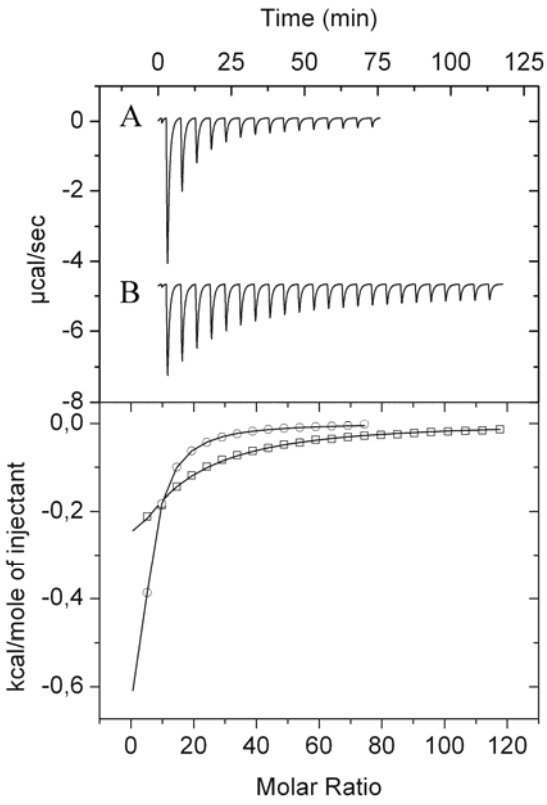


**Legend to Supplementary Figure 6) Microcalorimetric titration of McpS-LBR and its R183A mutant with acetate.** Upper panel: Raw data for the titration of 98 µM McpS-LBR (A) and McpS-LBR R183A (B) with 50 mM acetate. In both cases protein was in 5 mM Tris-HCl, 5 mM HEPES, 5 mM MES, pH 6.0. The injection volume was in both cases 12.8 µl. Lower panel: Integrated raw data after correction for dilution heats and normalization using ligand concentrations. ○ McpS-LBR ;□ McpS-LBR R183A. Data were fitted with the “One binding site model” of the MicroCal version of ORIGIN.

**Supplementary Figure 7)**

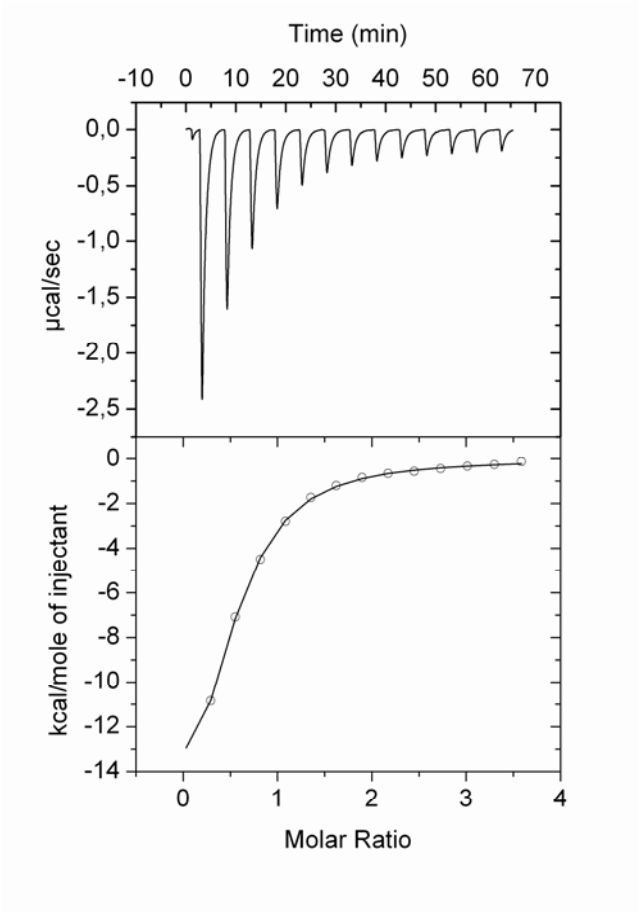


**Legend to Supplementary Figure 7) Microcalorimetric titration of McpS-LBR R183A with malate**. Upper panel: Raw data for the titration of 35 µM McpS-LBR with 12.8 µl aliquots of 1 mM malate. Lower panel: Integrated, concentration-normalized and dilution heat corrected raw data. Data were fitted using the "One binding site model" of the MicroCal version of ORIGIN. The thermodynamic data derived are: $\Delta H$ = -20.5 ± 0.7 kcal/mol and $K_D$ = 9,1 ± 0.4 µM.

**Supplementary Figure 8)**

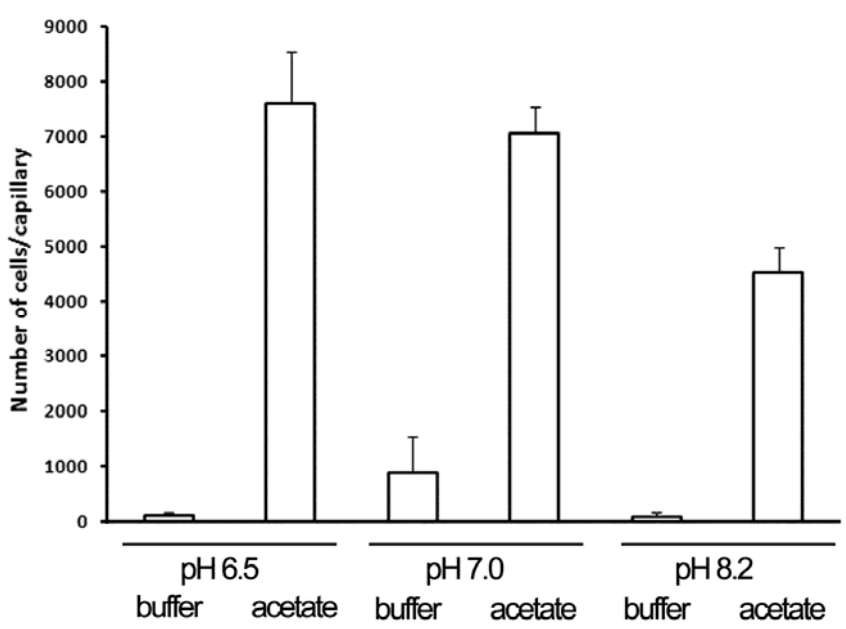


**Legend to Supplementary Figure 8) Effect of pH on chemotaxis of *P. putida* KT2440R to 50 mM acetate.** Quantitative capillary assays were conducted to measure chemotaxis of *P. putida* KT2440R towards 20 mM HEPES, 20 mM MES buffer at pH 6.5, 7 and pH 8.2. Subsequently taxis to 50 mM acetate solutions in those 3 buffer systems was monitored (the pH of the acetate solutions was verified and small pH deviations were corrected by the addition of diluted NaOH). Experiments were conducted in triplicates and results presented are the means and standard deviation of at least three individual experiments conducted in triplicates. A modified version of the capillary assay (Adler, (1973) J Gen Microbiology 98, 77-91) was used to quantify chemotaxis. In short, mineral salt medium (MS) supplemented with 10 mM succinate was inoculated with *P. putida* KT2440R and grown to early stationary phase at 30ºC with aeration. Cells were then diluted with MS to an $OD_{600}$ of 0.08 (corresponding to $10^6$-$10^7$ cells $ml^{-1}$). Capillary tubes (Microcaps, Drummond Scientific, USA) of 1 µl capacity were sealed at one end by melting over a flame. The capillary was then warmed over the flame and the open end inserted into attractant solution (20 mM HEPES, 20 mM MES buffer at pH values of 6.5, 7 and pH 8.2 with or without 50 mM acetate). About 0.15 ml of this suspension was placed into a small chamber formed by placing a v-shaped needle on a microscope slide. The system was then closed with a glass coverslip, avoiding the formation of air bubbles. A capillary tube was immersed into the cell suspension at its open end. After incubation for 15 min at room temperature, the open end of the capillary was then rinsed and placed into a microfuge tube containing 1 ml of MS buffer. The sealed end was broken and the contents were emptied into the tube. One hundred microliters of this cellular suspension was plated onto M9

medium plates supplement with 10 mM succinate and incubated at 30°C. Colonies were counted after 48 hours growth at 30°C. Note: *P. putida* KT2440R is a rifampicilin-resistant derivative of *P. putida* KT2440. Since the *mcpS* mutant was constructed using *P. putida* KT2440R, the rifampicilin-resistant wild type strain was used for chemotaxis assays.

**Supplementary Figure 9)**

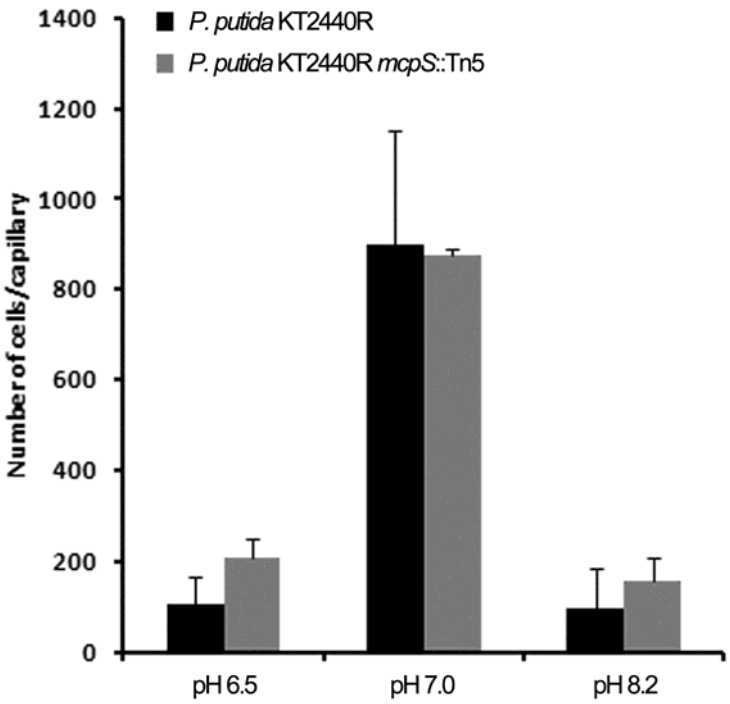


**Legend to Supplementary Figure 9) Chemotaxis response of *Pseudomonas putida* KT2440R and KT2440R *mcpS*::Tn5 strains to buffer at different pH**. Experiments were carried out as described for Supp. Fig. 8, except that the *mcpS* mutant strain was used.

**Supplementary Fig. 10)**

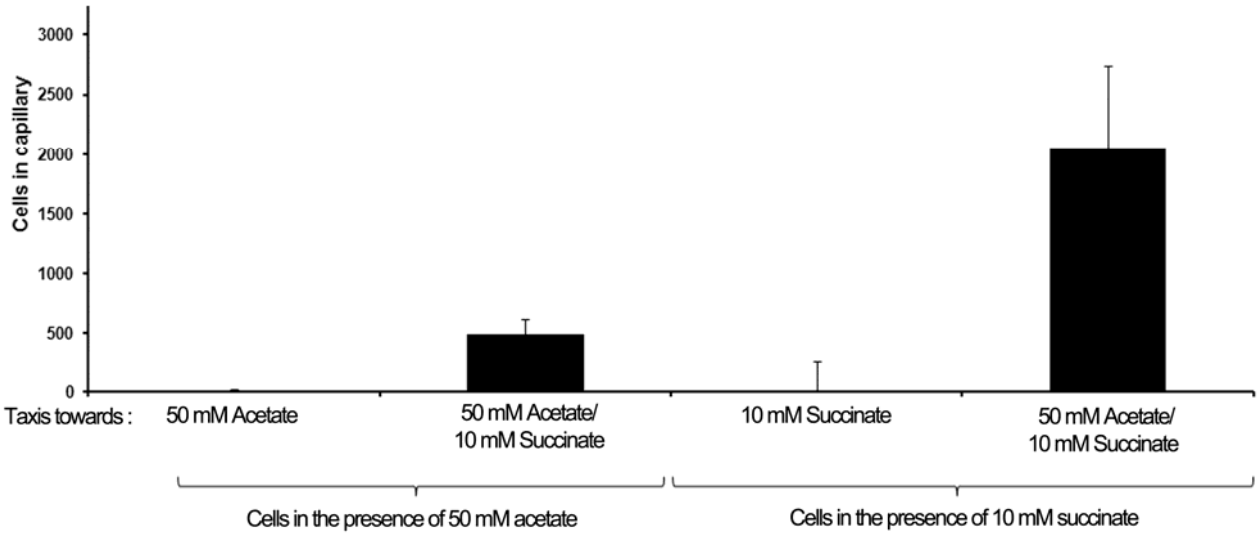


**Legend to Supplementary Figure 10) Evaluation of the influence of the presence of acetate on taxis to succinate and the presence of succinate on the presence of acetate.** *P. putida* KT2440R was grown to early stationary phase at 30ºC with aeration. Cells were then diluted with minimal slat medium to an $OD_{600}$ of 0.08 (corresponding to $10^6$-$10^7$ cells $ml^{-1}$) and acetate to a final concentration of 50 mM or succinate to a final concentration of 10 mM were added to the cellular suspension (note: the pH of the acetate and succinate mother solutions were adjusted the pH of the MS medium). Cells were then incubated at room temperature for 10 minutes. Quantitative capillary assays were conducted of acetate containing cells to acetate or to a mixture of acetate and succinate. Analogous experiments involved assays of succinate containing cells to succinate and to the mixture of acetate with succinate. The experiments were conducted as described in the legend to Supp. Figure 8. The data were corrected for background accumulation in capillaries containing buffer. Data shown are means and standard deviations from at least nine capillaries from experiments with at least three different bacterial cultures.

**Supplementary Fig. 11)**

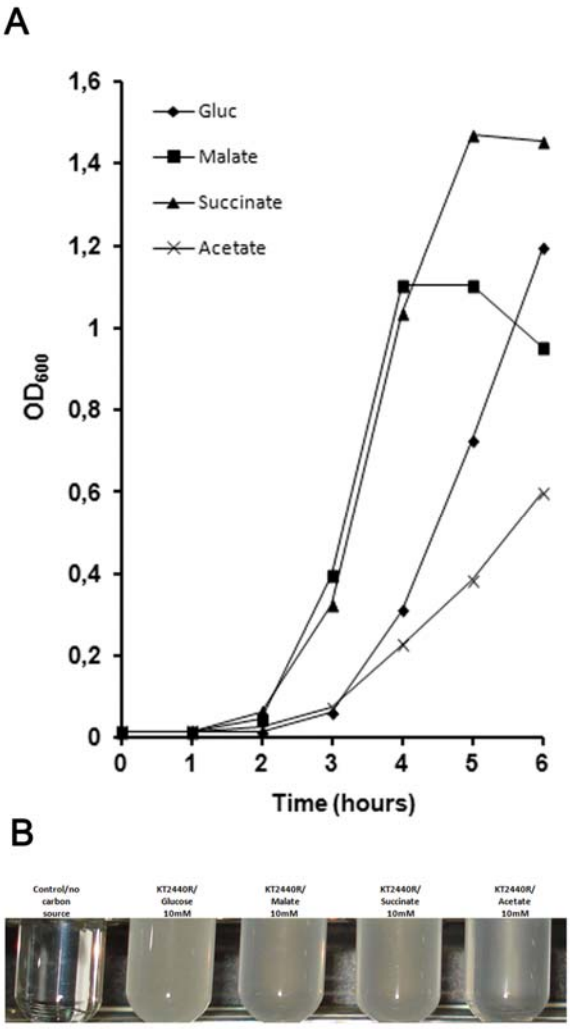


**Legend to Supplementary Figure 11) Growth of *P. putida* KT2440R in minimal medium supplemented with different carbon sources**. A) Growth curves. Cells were grown in minimal medium (M9) containing glucose, acetate, malate and succinate as carbon sources at a final concentration of 10 mM. Cells were inoculated into fresh media at an $OD_{600}$ of 0.015 from an M9+succinate stationary-phase culture. Growth at 30°C under agitation (200 rpm) was monitored by measuring $OD_{600}$. B) Image of growth culture tubes at the moment growth has ceased.

**Supplementary Table 1) Contacts between monomers A and B in the structure of McpS-LBR.**

| Amino acid/atom chain A | amino acid/atom chain B | Distance (Å) |
|---|---|---|
| Hydrogen bonds | | |
| Thr57/OG1 | Thr57/OG1 | 3.73 |
| Ser173/OG | Tyr169/OH | 3.29 |
| Ile184/O | Arg187/NH1 | 2.86 |
| Ala191/O | Asn70/ND2 | 3.52 |
| Glu192/OE1 | Arg134/NH2 | 3.72 |
| Tyr272/OH | Tyr272OH | 2.80 |
| Gln177/NE2 | Ser173/O | 3.80 |
| Gln177/NE2 | Gln177/OE1 | 3.06 |
| Arg187/NH1 | Ile184/O | 2.87 |
| Asn70/ND2 | Glu192/OE1 | 2.72 |
| Lys54/NZ | Asp269/OD1 | 3.23 |
| Salt bridges | | |
| Glu192/OE1 | Arg134/NH2 | 3.72 |
| Lys54/NZ | Asp269/OD1 | 3.23 |
| Lys54/NZ | Asp269/OD2 | 3.01 |

Hydrogen bonds were defined by a donor-acceptor distance of at least 3.8 Å and a donor acceptor angle of more than 90 degrees.

**Supplementary Table 2) Dissociation constants (in μM) determined from microcalorimetric titrations of native McpS-LBR and site-directed mutants R60A, R63A and R254A with different ligands.**

| | **wild type** | **R60A** | **R63A** | **R254A** |
|---|---|---|---|---|
| Malate | 8.5 ± 0.7[1] | No binding | No binding | No binding |
| Fumarate | 17 ± 2[1] | No binding | No binding | No binding |
| Oxaloacetate | 24 ± 6[1] | No binding | No binding | No binding |
| Succinate | 82 ± 3[1] | No binding | No binding | No binding |
| Butyrate | 92 ± 9[1] | No binding | No binding | 107 ± 17 |
| Citrate | 109 ± 14[1] | 500 ± 25 | 775 ± 60 | 813 ± 80 |
| Isocitrate | 337 ± 42[1] | No binding | No binding | No binding |

[1] Data are taken from Lacal *et al*. (2010) J. Biol. Chem. 285, 23126.

**Supplementary Table 3) Literature indicating high acetate concentrations in the natural habitat of *Pseudomonas*.**

| **Observation** | **Comment and literature references** |
|---|---|
| Acetogenesis under aerobic conditions | Growth on excess glucose or other highly assimilable carbon sources inhibits respiration, a behavior called the bacterial crabtree effect. As a consequence of the Crabtree effect, as much as 15% of the glucose can be excreted as acetate. As a consequence the acetate concentration in the growth medium increase to up to 10 mM – 35 mM in organisms as diverse as *E. coli* (El-Mansi and Holmes, (1989) J Gen Microbiol. 135:2875-83, Bulter et al. (2004) Proc Natl Acad Sci USA 101:2299-304), *Acetobacterium* spp. (Kim and Chang (2009) Bioresour Technol. 100:4527-30) or *Saccharomyces cerevisiae* (Aboca et al. (2012) Yeast 29:95-110). |
| Acetogenesis under anaerobic conditions | Under anaerobic conditions a branched TCA cycle occurs which forms succinyl-CoA by a reductive pathway and 2-ketoglutarate by an oxidative one. This branched form of the TCA cycle does not generate energy; instead it functions biosynthetically, producing precursor metabolites like acetate (Wolfe et al. (2005) Microbiol Mol Biol Rev. 69:12-50). |
| High abundance of acetate in sewage where it is considered as a major contaminant | Acetate is the primary product of acetogenesis in sewage ( Yu et al. Water Sci Technol. (2003) 48:69-75) and the dominating volatile fatty acid in wastewater (Raunkjaer et al (1997) Water Res. 31:2727-36) and is therefore considered as a contaminant. There is large number of studies which investigate acetate degradation in sewage waters (Wang and Ford (2009) Environ Sci Technol. 43:5921–5927, Toepfer et al. (2012) FEMS Microbiol Ecol. 81:163-71) |
| High acetate concentrations | *P. putida* KT2440 has a saprophytic lifestyle and acetate was found to be abundantly present in plant root tissues, where it accounted for around 1 % of the total organic carbon content of roots (Rentz et al. (2004) Environ Microbiol. 6:574-83). |
| High acetate concentrations in plant root exudates | *P. putida* KT2440 colonizes plant roots efficiently (Molina et al. (2000) Soil Biol. Biochem. 32:315–321) and was found to use organic acids present in root exudates as the primary carbon source during rhizosphere colonization (Lugtenberg et al. (2001) Annu. Rev. Phytopathol. 39:461–490). A study of Lucas-Garcia (2001) Phytochem Anal. 12:305-11) has shown that acetate is the most abundant organic acids present in exudates of *Lupinu albus* at concentration of around 1.5 mg/g root dry weight. These results are also consistent with a NMR study, which demonstrates that acetate is by far the most abundant organic compound in wheat root exudates (Fan et al. (2001) Phytochemistry 57:209-21). |

**Supplementary Table 4) Oligonucleotides used for the construction of McpS-LBR mutants.**

| Name | sequence | Construction of mutant |
|---|---|---|
| | | |
| R60A | 5’-TCACCGATCTAGCCATTGCGCGCCTGCA -3’, | R60A |
| R63A | 5’-TCTACGCATTGCGGCCCTGCAGTACATGA-3’, | R63A |
| R254A | 5’-ACATCACCACCTCGGCCGCCGAAATGAC-3’ | R254A |
| | | |
| R183Af1 | 5’-GACCGTAGCAACCATATGGGCGATATTGG-3’ | R183A |
| R183Ar1 | 5’-CACATCGATG*GC*TACCTGCAGCAG-3` | R183A |
| R183Af2 | 5’-CCTGCAGGCTGGGATCCTGTCAGCTCTCGAT-3’ | R183A |
| R183Ar2 | 5`- CTGCTGCAGGTA*GC*CATCGATGTG-3’ | R183A |

# Supplementary analysis 1)

**Secondary structure prediction and three dimensional homology modeling of the ligand binding regions of 50 randomly selected cluster II chemoreceptors.** The transmembrane regions of these receptors were predicted by the DAS algorithm (Cserzo et al. (1997) Prot. Eng. 10 673-676) and the sequence fragment in between both transmembrane regions, comprising the ligand binding region, were submitted to the consensus secondary structure prediction algorithm (http://npsa-pbil.ibcp.fr/cgi-bin/npsa_automat.pl?page=/NPSA/npsa_seccons.html). Obtained profiles were then classified as belonging to the double PDC like fold or the McpS-LBR like fold. All ligand binding regions were submitted to 3D homology modeling algorithm using CPH models (http://www.cbs.dtu.dk/services/CPHmodels/, Nielsen et al. (2010) Nucleic Acids Research 38, doi:10.1093/nar/gkq535) and in cases where modeling was possible, the resulting models are shown. The phylogenetic characteristics of the corresponding strains are indicated. At the beginning of this document the 3D structures and the secondary structure profiles of two reference proteins for double PDC and McpS-like domains are shown..

Codes for secondary structure predictions: blue bar: alpha helix, red bar: beta strand, pink bar: coil

Classification of chemoreceptors according to the size of their ligand binding region. Figure taken from Lacal et al. (2010) Env. Microbiol. 12, 2873.

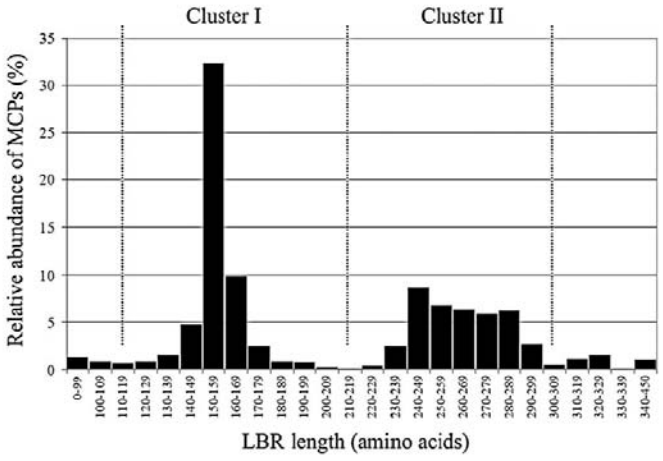


**Fig. 6.** Classification of MCP sequences according to the size of the LBR. This study is based on the totality of MCPs that show topology Ia (2386 of bacterial origin and 50 of archaea). This topology is predominant in bacteria and archaea. The LBR of proteins of this topology is flanked by two TM regions and therefore the size of the LBR can be determined precisely.

**Reference structures and secondary structure prediction output for a double PDC domain and for the McpS-lignad binding region**

1. **Double PDC domain: Crystal Structure of the extracellular domain of the putative histidine kinase from** *Methanosarcina mazei* **(pdb: 3**Lia, Zhang and Hendrickson , 2010, J Mol Biol. 400:335-53) and the secondary structure profile.


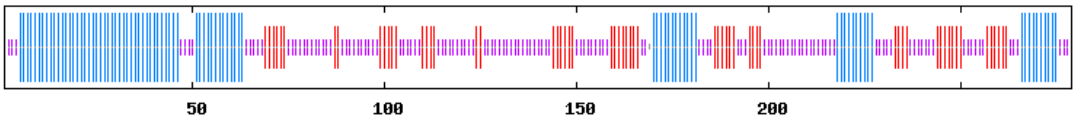


**2. Structure and secondary structure prediction for McpS-LBR of *P. putida* KT2440.**

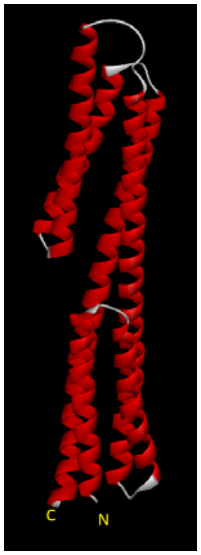


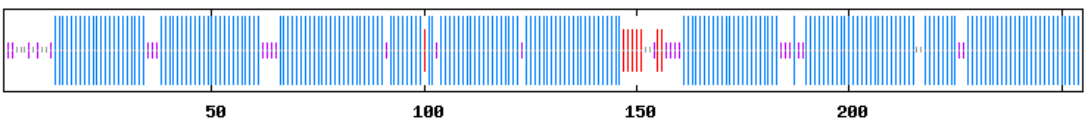

**Ligand binding regions of the 50 selected chemoreceptors that match the secondary structure profile of double PDC sensor domain fold. When available, 3D homology models of these domains or fragments thereof are shown.**

1) >uniprot|Q0AV12|Q0AV12_SYNWW Putative methyl-accepting chemotaxis sensory transducer precursor [Syntrophomonas wolfei subsp. wolfei str. Goettingen]
Bacteria › Firmicutes › Clostridia › Clostridiales › Syntrophomonadaceae › Syntrophomonas

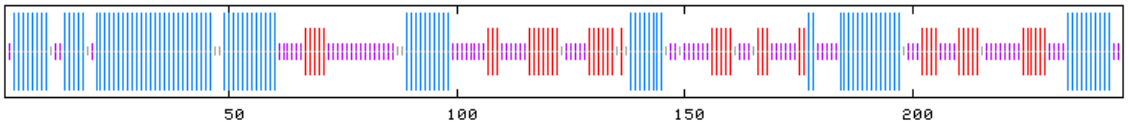



2) >uniprot|Q9KSG7|Q9KSG7_VIBCH Methyl-accepting chemotaxis protein [Vibrio cholerae O1 biovar El Tor str. N16961
Bacteria › Proteobacteria › Gammaproteobacteria › Vibrionales › Vibrionaceae › Vibrio

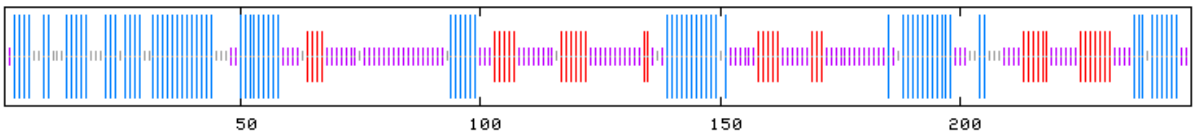


3) >uniprot|Q314Z2|Q314Z2_DESDG Methyl-accepting chemotaxis sensory transducer [Desulfovibrio desulfuricans subsp. desulfuricans str. G20]
Bacteria › Proteobacteria › Deltaproteobacteria › Desulfovibrionales › Desulfovibrionaceae › Desulfovibrio

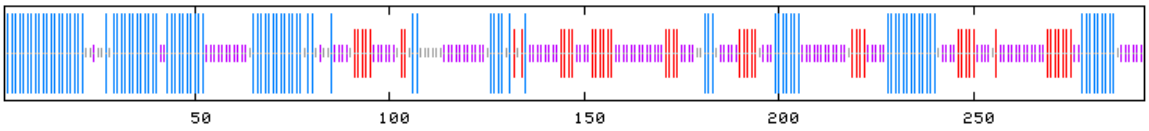


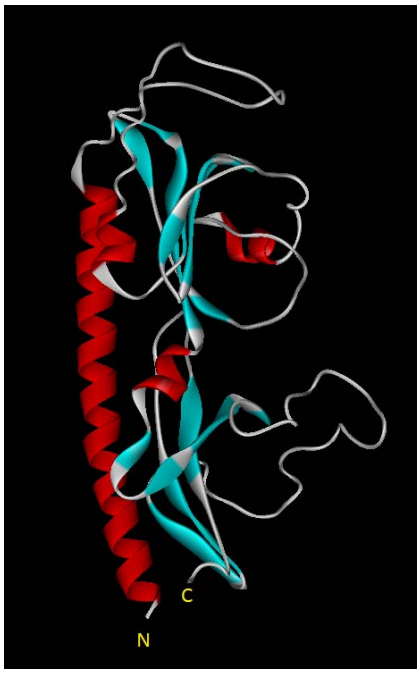


4) >tr|H3SL86|H3SL86_9BACL Methyl-accepting chemotaxis protein OS=Paenibacillus dendritiformis C454 GN=PDENDC454_21604 PE=4 SV=1
Bacteria › Firmicutes › Bacillales › Paenibacillaceae › Paenibacillus

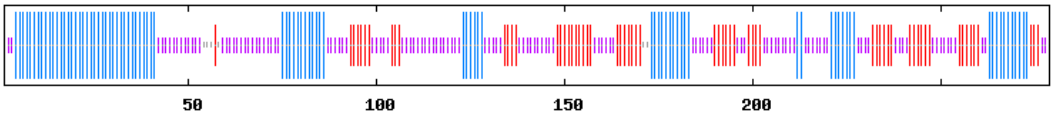



5) >tr|A6LJU3|A6LJU3_THEM4 Methyl-accepting chemotaxis sensory transducer OS=Thermosipho melanesiensis (strain BI429 / DSM 12029) GN=Tmel_0322 PE=4 SV=1
Bacteria › Thermotogae › Thermotogales › Thermotogaceae › Thermosipho

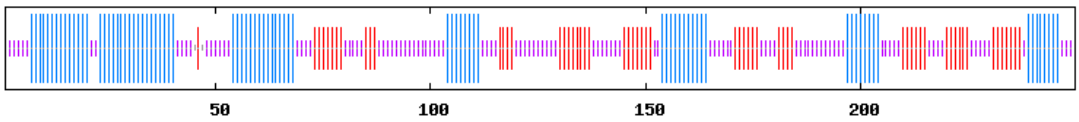


6) >tr|A5N103|A5N103_CLOK5 Predicted methyl-accepting chemotaxis protein OS=Clostridium kluyveri (strain ATCC 8527 / DSM 555 / NCIMB 10680) GN=CKL_2787 PE=4 SV=1
Bacteria › Firmicutes › Clostridia › Clostridiales › Clostridiaceae › Clostridium

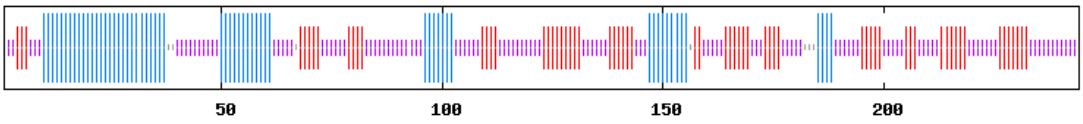


7)>tr|E8UWG7|E8UWG7_THEBF Chemotaxis sensory transducer OS=Thermoanaerobacter brockii subsp. finnii (strain ATCC 43586 / DSM 3389 / AKO-1) GN=Thebr_1886 PE=4 SV=1
Bacteria › Firmicutes › Clostridia › Thermoanaerobacterales › Thermoanaerobacteriaceae › Thermoanaerobacter

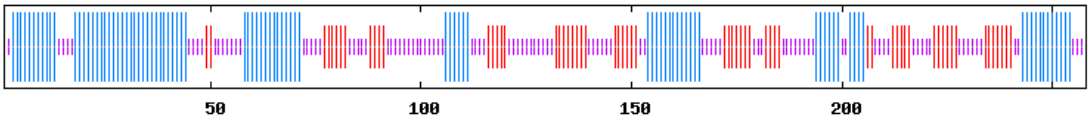


8) >string|326423.RBAM_028290|326423.RBAM_028290 TlpB [Bacillus amyloliquefaciens FZB42]
Bacteria › Firmicutes › Bacillales › Bacillaceae › Bacillus

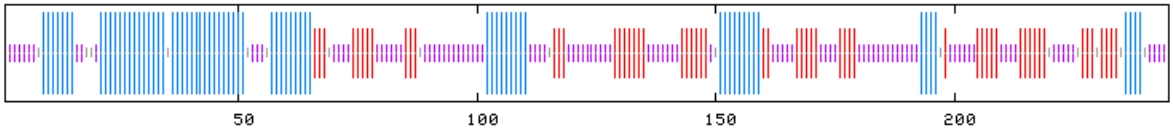



9) >uniprot|A4J3R2|A4J3R2_9FIRM Methyl-accepting chemotaxis sensory transducer precursor [Desulfotomaculum reducens MI-1]
Bacteria › Firmicutes › Clostridia › Clostridiales › Peptococcaceae › Desulfotomaculum

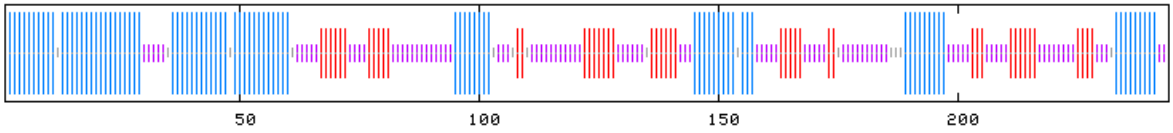



10) >uniprot|A6WDS8|A6WDS8_KINRA Methyl-accepting chemotaxis sensory transducer precursor [Kineococcus radiotolerans SRS30216]
Bacteria › Actinobacteria › Actinobacteridae › Actinomycetales › Kineosporiineae › Kineosporiaceae › Kineococcus

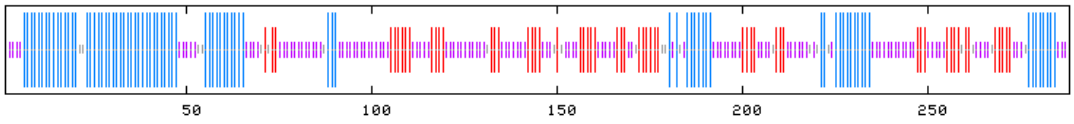


11) uniprot|Q0BGB8|Q0BGB8_BURCM Methyl-accepting chemotaxis sensory transducer precursor [Burkholderia ambifaria AMMD]
Bacteria › Proteobacteria › Betaproteobacteria › Burkholderiales › Burkholderiaceae › Burkholderia › Burkholderia cepacia complex

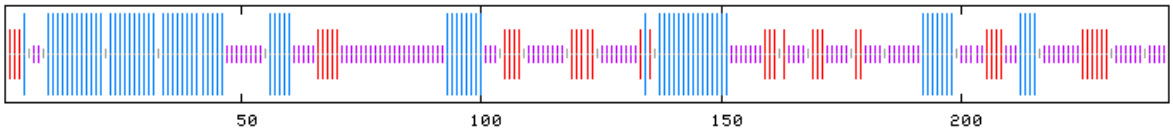


**No 3D modelization possible**

12) >uniprot|A1S1I6|A1S1I6_SHEAM Putative methyl-accepting chemotaxis sensory transducer precursor [Shewanella amazonensis SB2B]
Bacteria › Proteobacteria › Gammaproteobacteria › Alteromonadales › Shewanellaceae › Shewanella

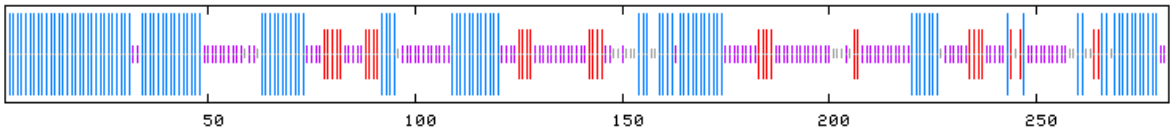


**No modelling possible**

13) >uniprot|A6TSC5|A6TSC5_9CLOT Methyl-accepting chemotaxis sensory transducer precursor [Alkaliphilus metalliredigens QYMF]
Bacteria › Firmicutes › Clostridia › Clostridiales › Clostridiaceae › Alkaliphilus

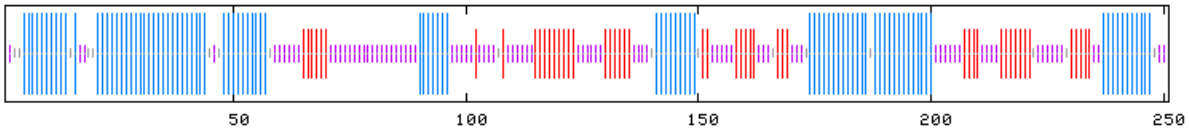


**No modelling possible**

14) >uniprot|A3QAH0|A3QAH0_SHELP Methyl-accepting chemotaxis sensory transducer precursor [Shewanella loihica PV-4]
Bacteria › Proteobacteria › Gammaproteobacteria › Alteromonadales › Shewanellaceae › Shewanella

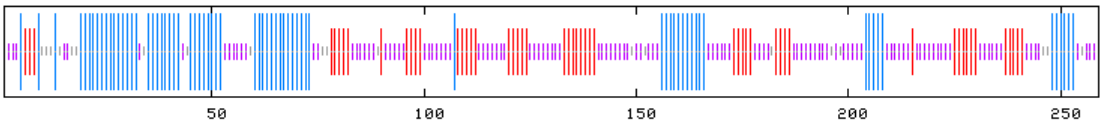

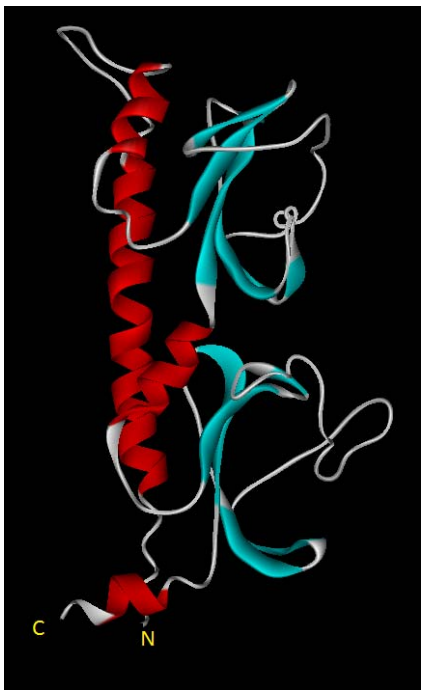


15) >tr|B3IZY6|B3IZY6_BACAN Methyl-accepting chemotaxis protein OS=Bacillus anthracis Tsiankovskii-I GN=BATI_3176 PE=4 SV=1
Bacteria › Firmicutes › Bacillales › Bacillaceae › Bacillus › Bacillus cereus group

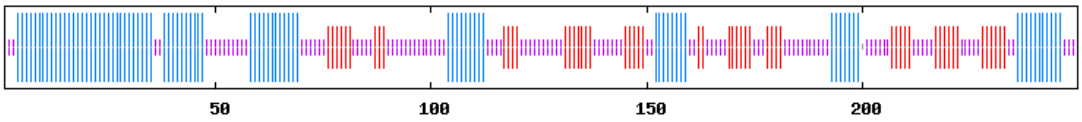


16) >tr|B7R938|B7R938_9THEO Methyl-accepting chemotaxis protein signaling domain protein OS=Carboxydibrachium pacificum DSM 12653 GN=CDSM653_848 PE=4 SV=1

Bacteria › Firmicutes › Clostridia › Thermoanaerobacterales › Thermoanaerobacteriaceae › Caldanaerobacter

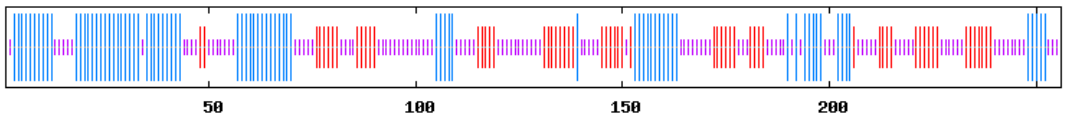


17) >uniprot|Q63G86|Q63G86_BACCZ Methyl-accepting chemotaxis protein [Bacillus cereus E33L]
Bacteria › Firmicutes › Bacillales › Bacillaceae › Bacillus › Bacillus cereus group

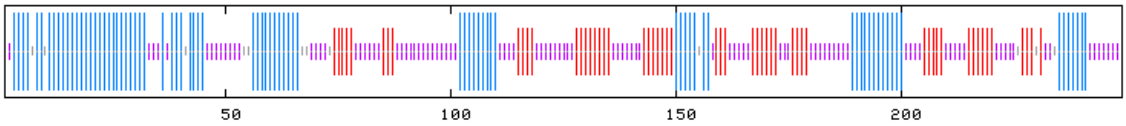


18) uniprot|Q8DLC7|Q8DLC7_SYNEL methyl-accepting chemotaxis protein [Thermosynechococcus elongatus BP-1]
Bacteria › Cyanobacteria › Chroococcales › Thermosynechococcus

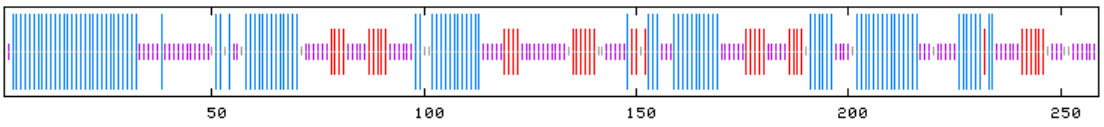



19) >uniprot|A1WD99|A1WD99_ACISJ Methyl-accepting chemotaxis sensory transducer precursor [Acidovorax sp. JS42]
Bacteria › Proteobacteria › Betaproteobacteria › Burkholderiales › Comamonadaceae › Acidovorax

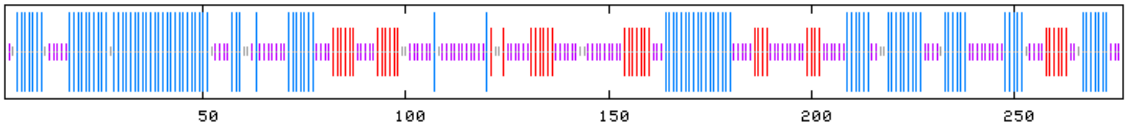

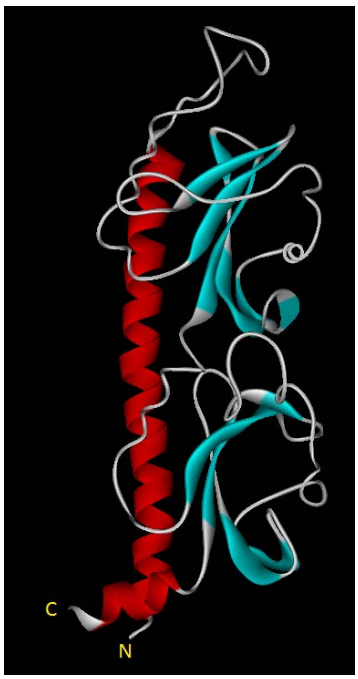


20) >uniprot|Q3ADB4|Q3ADB4_CARHZ Methyl-accepting chemotaxis protein [Carboxydothermus hydrogenoformans Z-2901]
Bacteria › Firmicutes › Clostridia › Thermoanaerobacterales › Thermoanaerobacteriaceae › Carboxydothermus

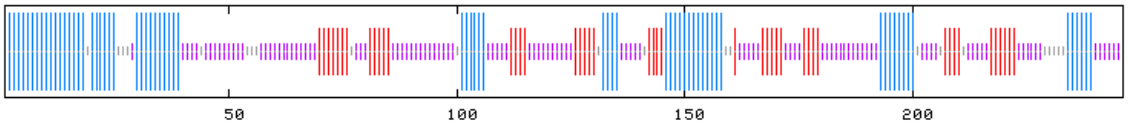


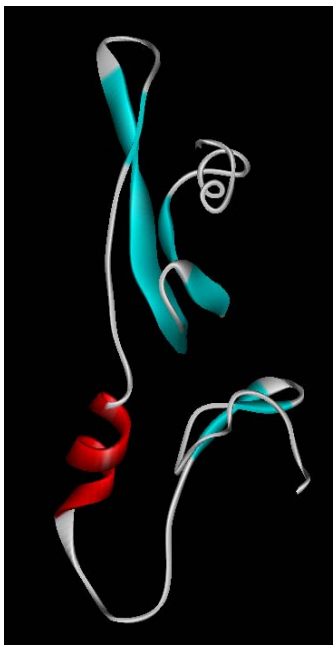

21) >tr|A6VAX7|A6VAX7_PSEA7 Chemotactic transducer PctA OS=Pseudomonas aeruginosa (strain PA7) GN=pctA PE=4 SV=1
Bacteria › Proteobacteria › Gammaproteobacteria › Pseudomonadales › Pseudomonadaceae › Pseudomonas

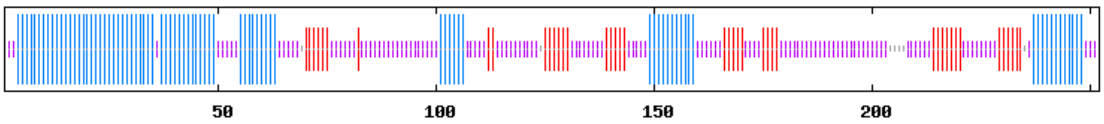


22) >tr|A6EVV0|A6EVV0_9ALTE Methyl-accepting chemotaxis protein OS=Marinobacter algicola DG893 GN=MDG893_07065 PE=4 SV=1
Bacteria › Proteobacteria › Gammaproteobacteria › Alteromonadales › Alteromonadaceae › Marinobacter

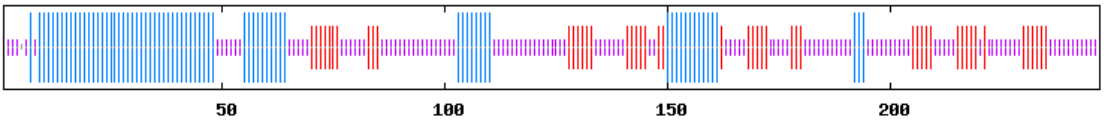


**No modelling possible**

23) >tr|E6XJV8|E6XJV8_SHEP2 Methyl-accepting chemotaxis sensory transducer with Cache sensor OS=Shewanella putrefaciens (strain 200) GN=Sput200_1889 PE=4 SV=1
Bacteria › Proteobacteria › Gammaproteobacteria › Alteromonadales › Shewanellaceae › Shewanella

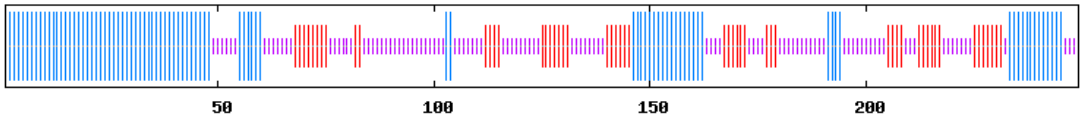


24)>tr|H2G1L7|H2G1L7_OCESG Methyl-accepting chemotaxis sensory transducer OS=Oceanimonas sp. (strain GK1) GN=GU3_04320 PE=4 SV=1
Bacteria › Proteobacteria › Gammaproteobacteria › Aeromonadales › Aeromonadaceae › Oceanimonas

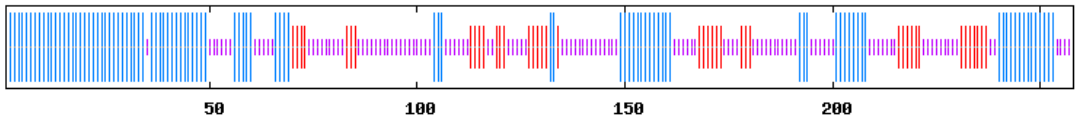


25)>tr|F3BIJ7|F3BIJ7_PSEHA Putative chemotactic transducer OS=Pseudoalteromonas haloplanktis ANT/505 GN=PH505_ap00180 PE=4 SV=1
Bacteria › Proteobacteria › Gammaproteobacteria › Alteromonadales › Pseudoalteromonadaceae › Pseudoalteromonas

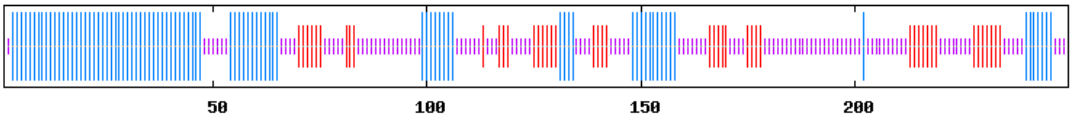


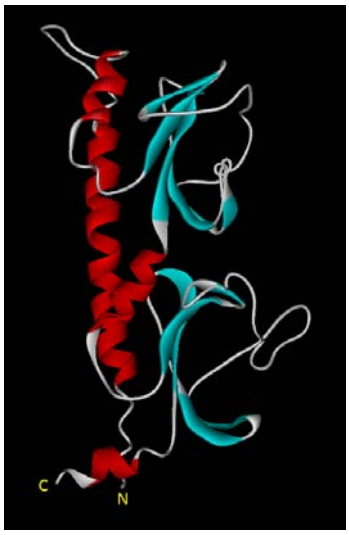


26) >tr|A4SK06|A4SK06_AERS4 Methyl-accepting chemotaxis protein OS=Aeromonas salmonicida (strain A449) GN=ASA_1106 PE=4 SV=1
Bacteria › Proteobacteria › Gammaproteobacteria › Aeromonadales › Aeromonadaceae › Aeromonas

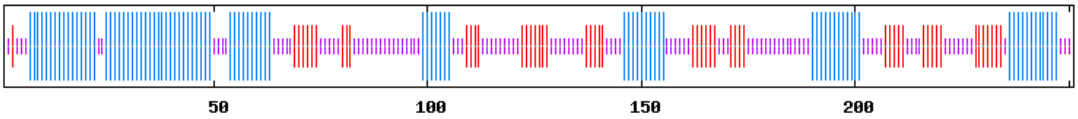



27) >tr|Q9KAL2|Q9KAL2_BACHD Methyl-accepting chemotaxis protein OS=Bacillus halodurans (strain ATCC BAA-125 / DSM 18197 / FERM 7344 / JCM 9153 / C-125) GN=BH2275 PE=4 SV=1

Bacteria › Firmicutes › Bacillales › Bacillaceae › Bacillus

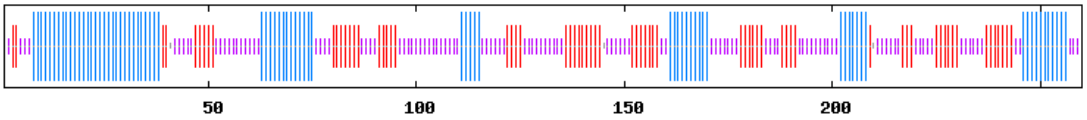


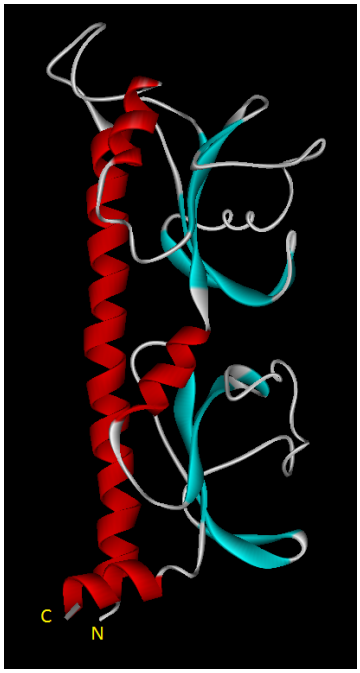

**Ligand binding regions of the 50 selected chemoreceptors that match the secondary structure profile of the McpS-LBR. When available, 3D homology models of these domains or fragments thereof are shown.**

1) uniprot|A0KGQ7|A0KGQ7_AERHH Putative chemotaxis transducer [Aeromonas hydrophila subsp. hydrophila ATCC 7966]
Bacteria › Proteobacteria › Gammaproteobacteria › Aeromonadales › Aeromonadaceae › Aeromonas

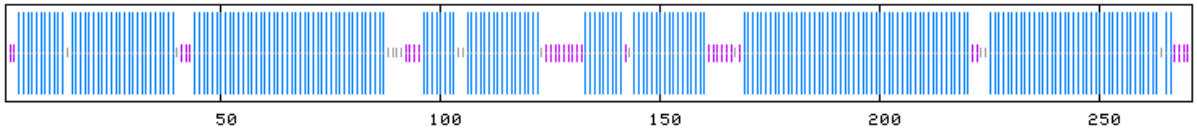


2) >tr|A7K1V8|A7K1V8_VIBSE Methyl-accepting chemotaxis protein OS=Vibrio sp. (strain Ex25) GN=VEA_001468 PE=4 SV=1
Bacteria › Proteobacteria › Gammaproteobacteria › Vibrionales › Vibrionaceae › Vibrio

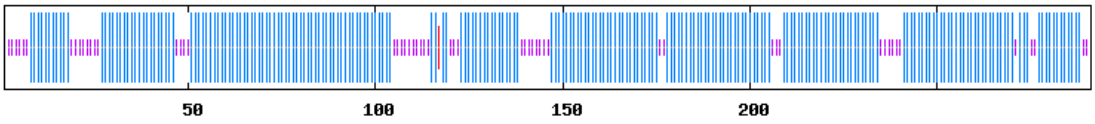


3) uniprot|Q9RYG4|Q9RYG4_DEIRA methyl-accepting chemotaxis-related protein [Deinococcus radiodurans R1]
Bacteria › Deinococcus-Thermus › Deinococci › Deinococcales › Deinococcaceae › Deinococcus

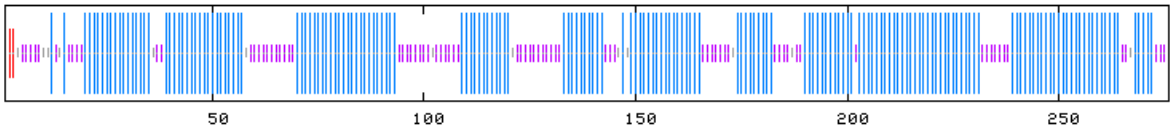


**4)** uniprot|A1U770|A1U770_MARAV Methyl-accepting chemotaxis sensory transducer [Marinobacter aquaeolei VT8]
Bacteria › Proteobacteria › Gammaproteobacteria › Alteromonadales › Alteromonadaceae › Marinobacter

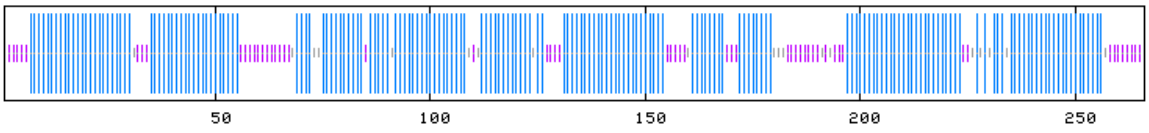


**5)** uniprot|Q8Y1L9|Q8Y1L9_RALSO Putative twitching motility transmembrane protein [Ralstonia solanacearum GMI1000]
Bacteria › Proteobacteria › Betaproteobacteria › Burkholderiales › Burkholderiaceae › Ralstonia

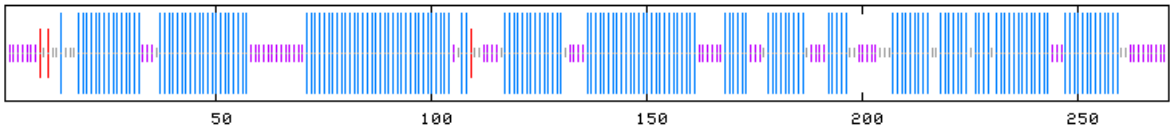

6) uniprot|Q07HJ2|Q07HJ2_RHOP5 Methyl-accepting chemotaxis sensory transducer precursor [Rhodopseudomonas palustris BisA53]
Bacteria › Proteobacteria › Alphaproteobacteria › Rhizobiales › Bradyrhizobiaceae › Rhodopseudomonas

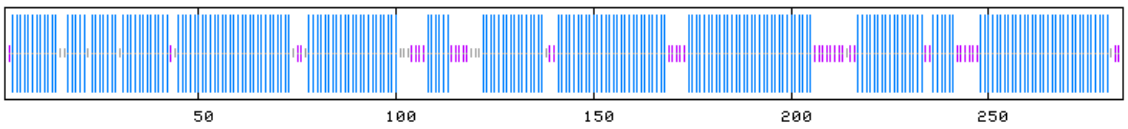


7) >tr|Q1IFB1|Q1IFB1_PSEE4 Putative methyl-accepting chemotaxis transducer OS=Pseudomonas entomophila (strain L48) GN=PSEEN0717 PE=4 SV=1
Bacteria › Proteobacteria › Gammaproteobacteria › Pseudomonadales › Pseudomonadaceae › Pseudomonas

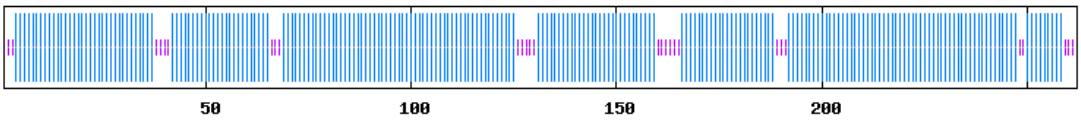


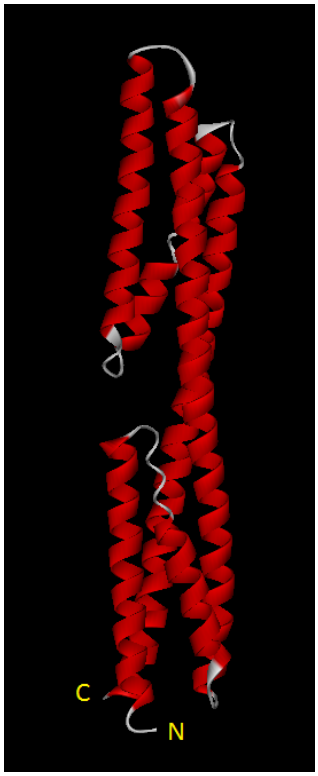


8) >tr|G2L0T0|G2L0T0_PSEAI Putative chemotaxis transducer OS=Pseudomonas aeruginosa M18 GN=PAM18_5187 PE=4 SV=1
Bacteria › Proteobacteria › Gammaproteobacteria › Pseudomonadales › Pseudomonadaceae › Pseudomonas

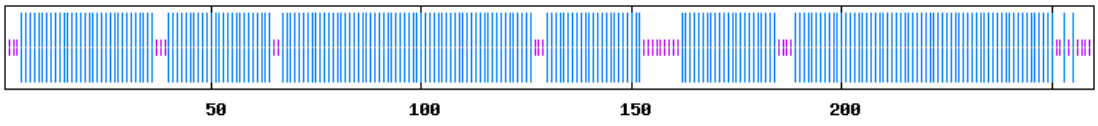

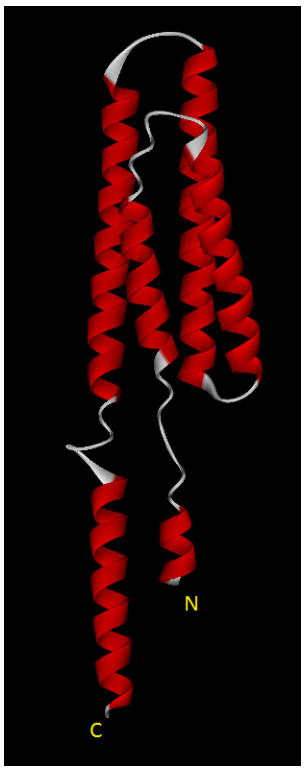


9) tr|Q1QPB9|Q1QPB9_NITHX Methyl-accepting chemotaxis sensory transducer OS=Nitrobacter hamburgensis (strain X14 / DSM 10229) GN=Nham_1080 PE=4 SV=1
Bacteria › Proteobacteria › Alphaproteobacteria › Rhizobiales › Bradyrhizobiaceae › Nitrobacter

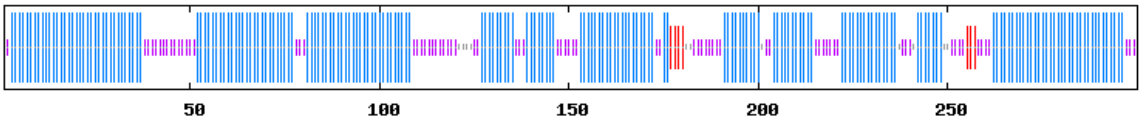


10) >uniprot|A5EAD2|A5EAD2_BRASB Putative methyl-accepting chemotaxis receptor/sensory transducer [Bradyrhizobium sp. BTAi1]
Bacteria › Proteobacteria › Alphaproteobacteria › Rhizobiales › Bradyrhizobiaceae › Bradyrhizobium

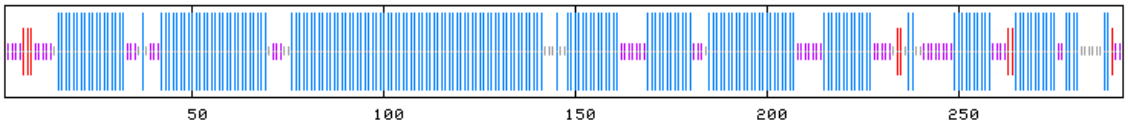


11) >tr|A9W2P9|A9W2P9_METEP Chemotaxis sensory transducer OS=Methylobacterium extorquens (strain PA1) GN=Mext_1454 PE=4 SV=1
Bacteria › Proteobacteria › Alphaproteobacteria › Rhizobiales › Methylobacteriaceae › Methylobacterium

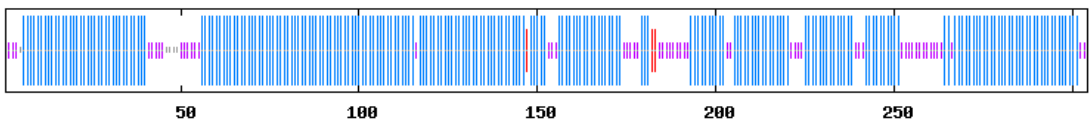


12) >tr|Q4KIL8|Q4KIL8_PSEF5 Methyl-accepting chemotaxis sensory transducer OS=Pseudomonas fluorescens (strain Pf-5 / ATCC BAA-477) GN=PFL_0778 PE=4 SV=1

Bacteria › Proteobacteria › Gammaproteobacteria › Pseudomonadales › Pseudomonadaceae › Pseudomonas

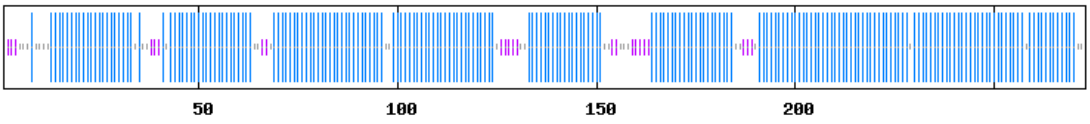


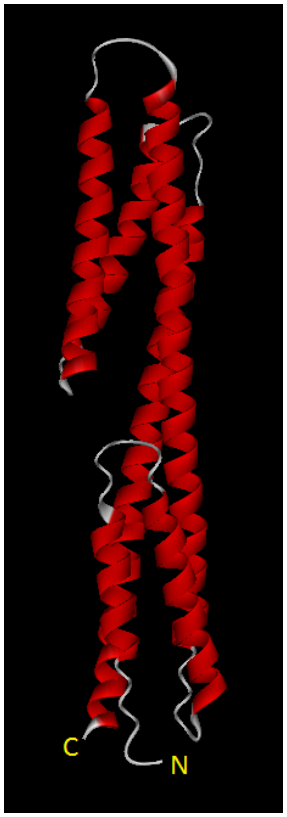


13) >tr|Q2W0L7|Q2W0L7_MAGSA Methyl-accepting chemotaxis protein OS=Magnetospirillum magneticum (strain AMB-1 / ATCC 700264) GN=amb3804 PE=4 SV=1,
Bacteria › Proteobacteria › Alphaproteobacteria › Rhodospirillales › Rhodospirillaceae › Magnetospirillum

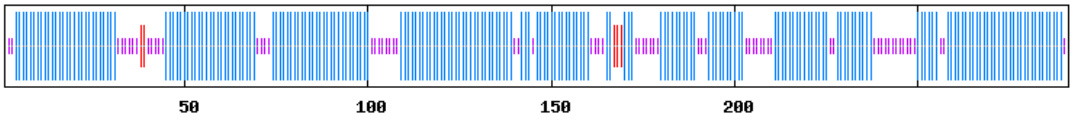


14) >tr|D3P1U9|D3P1U9_AZOS1 Methyl-accepting chemotaxis protein OS=Azospirillum sp. (strain B510) GN=AZL_a10970 PE=4 SV=1
Bacteria › Proteobacteria › Alphaproteobacteria › Rhodospirillales › Rhodospirillaceae › Azospirillum

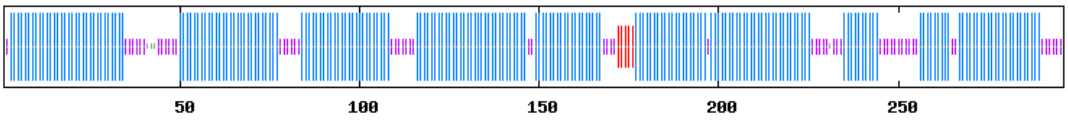


15) >tr|G2ZPS4|G2ZPS4_9RALS Type IV pilus transmembrane protein PilJ,twitching motility, Methyl-accepting chemotaxis protein OS=blood disease bacterium R229 GN=pilJ PE=4 SV=1

Bacteria › Proteobacteria › Betaproteobacteria › Burkholderiales › Burkholderiaceae › Ralstonia

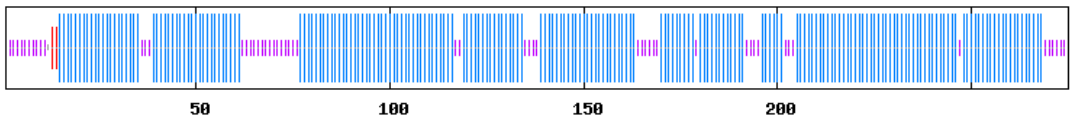


16) >tr|B3R317|B3R317_CUPTR TWITCHING MOTILITY TRANSMEMBRANE PROTEIN, Methyl-accepting chemotaxis protein OS=Cupriavidus taiwanensis (strain R1 / LMG 19424) GN=pilJ PE=4 SV=1
Bacteria › Proteobacteria › Betaproteobacteria › Burkholderiales › Burkholderiaceae › Cupriavidus

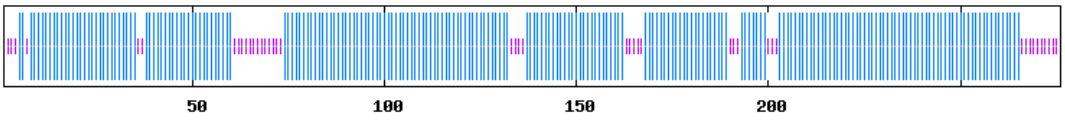


17) >tr|D8DDK7|D8DDK7_COMTE Methyl-accepting chemotaxis sensory transducer OS=Comamonas testosteroni S44 GN=CTS44_24573 PE=4 SV=1
Bacteria › Proteobacteria › Betaproteobacteria › Burkholderiales › Comamonadaceae › Comamonas

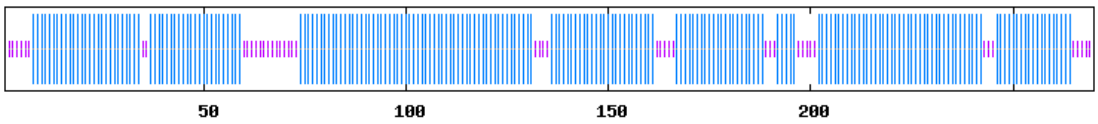


18) >tr|A7BZF5|A7BZF5_9GAMM Methyl-accepting chemotaxis sensory transducer OS=Beggiatoa sp. PS GN=BGP_1625 PE=4 SV=1
Bacteria › Proteobacteria › Gammaproteobacteria › Thiotrichales › Thiotrichaceae › Beggiatoa

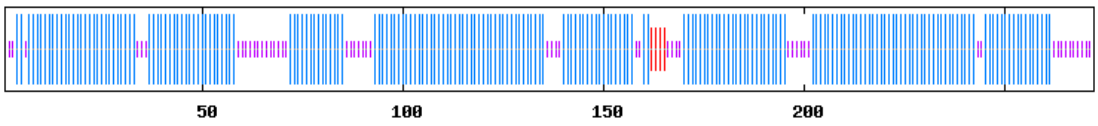


19)>tr|D3RVN3|D3RVN3_ALLVD Methyl-accepting chemotaxis sensory transducer OS=Allochromatium vinosum (strain ATCC 17899 / DSM 180 / NBRC 103801 / D) GN=Alvin_0193 PE=4 SV=1
Bacteria › Proteobacteria › Gammaproteobacteria › Chromatiales › Chromatiaceae › Allochromatium

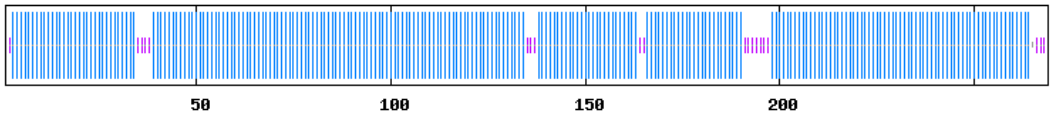


20)>tr|F7NA63|F7NA63_XYLFA Methyl-accepting chemotaxis protein Tar OS=Xylella fastidiosa EB92.1 GN=tar PE=4 SV=1
Bacteria › Proteobacteria › Gammaproteobacteria › Xanthomonadales › Xanthomonadaceae › Xylella

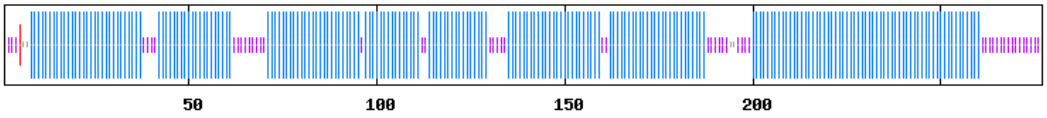


21) >tr|D4SXS5|D4SXS5_9XANT Pilus biogenesis protein OS=Xanthomonas fuscans subsp. aurantifolii str. ICPB 11122 GN=pilJ PE=4 SV=1

Bacteria › Proteobacteria › Gammaproteobacteria › Xanthomonadales › Xanthomonadaceae › Xanthomonas

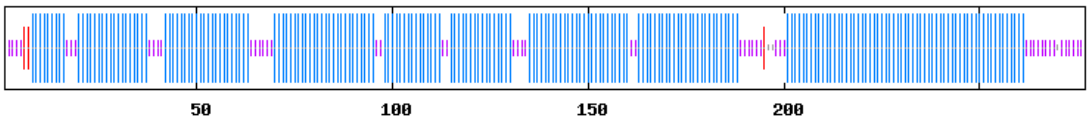


22) >tr|E8TQJ1|E8TQJ1_ALIDB Chemotaxis sensory transducer OS=Alicycliphilus denitrificans (strain JCM 14587 / BC) GN=Alide_3630 PE=4 SV=1
Bacteria › Proteobacteria › Betaproteobacteria › Burkholderiales › Comamonadaceae › Alicycliphilus

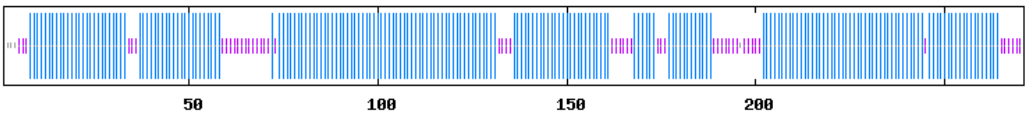


23) >tr|Q478V7|Q478V7_DECAR Chemotaxis sensory transducer OS=Dechloromonas aromatica (strain RCB) GN=Daro_3896 PE=4 SV=1
Bacteria › Proteobacteria › Betaproteobacteria › Rhodocyclales › Rhodocyclaceae › Dechloromonas